Development of a hydrodynamic model to investigate near field and regional connectivity around Okehampton Bay

Clothilde Langlais, John Andrewartha, Mike Herzfeld

January 2021

FRDC Project No 2018-119

ISBN 978-0-6482348-1-4

Development of a hydrodynamic model to investigate near field and regional connectivity around Okehampton Bay

FRDC 2018-119

2021

Researcher Contact Details

Name:	Brad Evans
Address:	Tassal Group Limited
Phone:	0414 675 293
Fax:	
Email:	Brad.Evans@tassal.com.au

FRDC Contact Details

Address:	25 Geils Court
	Deakin ACT 2600
Phone:	02 6285 0400
Fax:	02 6285 0499
Email:	frdc@frdc.com.au
Web:	www.frdc.com.au

In submitting this report, the researcher has agreed to FRDC publishing this material in its edited form.

Contents

Tables

Figures

Acknowledgments

This work has been funded by the Tassal project ‘Okehampton Bay Modelling’.

For calibration and validation purposes, Tassal provided historical observations: temperature and salinity records from data loggers and profiling buoys.

EPA and Tassal also provided data from the ongoing far-field ambient monitoring program that consists of seven Broadscale Environmental Monitoring (BEMP) sites.

As in-kind contributions to this project, Tassal also deployed three moorings within the local region hosting surface and bottom instruments.

Executive Summary

The study aims to satisfy the regulatory requirements of Environmental Licence 10172/2 from the Tasmanian EPA around Tassal's use of Okehampton Bay for salmonoid aquaculture, particularly the possible fate of material released within Okehampton Bay into the receiving environment. To achieve that objective, the CSIRO Coastal Environment Modelling team (CEM team) developed a hydrodynamic model to investigate the far field and regional hydrodynamic connectivity around Okehampton Bay and the Mercury Passage surrounds, hereafter referred to as the OKE model.

For the first stage of this project, a pilot model was developed and run over the 2016-2017 period. Calibration and validation of the OKE model against observations was provided in the second phase of this project. This report provides details of the development of the calibrated model. The observations provided were sufficient to calibrate the model to a satisfactory standard.

The calibrated OKE model was also used to provide information of the far-field connectivity characteristics between the Okehampton Bay Tassal lease site and nearby regions. The use of point source passive tracers is the most informative metric to understand where and in what quantities tracers are transported by the currents around the lease. In Okehampton Bay, the highest concentrations resulting from tracer released at the bottom are found near the source point at the bottom of the lease. At the surface, the tracer tends to be trapped along Okehampton Beach (north-east part of Okehampton Bay). Further afield, the plume of high tracer concentration is trapped along the coast in shallow areas. The high concentration plume is transported almost equally northward and southward of the lease, with a median tracer concentration of $8x10^{-4}$ kg/m^3 at a 5 km distance from the 1 kg/s source point. At a larger scale, the plume tends to deviate southward toward Triabunna, Orford and the Mercury Passage, and only reach Little Swanport towards the north. This behaviour is characteristic of the August 2018-July 2019 studied period. Results from the pilot model over the 2016-2017 period suggest that there is some interannual variability associated with the northward/southward extend of the plume.

From a circulation point of view, the local currents push the passive tracer less often to the south than to the north. However, the southward meandering circulation can deflect the tracer towards the south, offshore of the lease. Moreover, as the tracer stays trapped for longer periods near Triabunna, Orford and Spring Beach than in Plain Place Bay, the median concentration south of the lease is higher than north of the lease in 2018-2019.

This report is solely based on hydrodynamic modelling and passive tracer dispersion (with no decay applied to the tracer). To understand the impact of marine farming in Okehampton Bay, on receiving water quality and sediment dynamics, a calibrated biogeochemical model would be required.

Keywords: *Hydrodynamics, connectivity, Modelling, Okehampton Bay*

1. Introduction

1.1 Aim

The objective of this project is to develop a hydrodynamic model to investigate the far field and regional hydrodynamic connectivity around Okehampton Bay and Mercury Passage surrounds. The study aims to satisfy the regulatory requirements of Environmental Licence 10172/2 from the Tasmanian EPA around Tassal's use of Okehampton Bay for salmonoid aquaculture, particularly the possible fate of material released within Okehampton Bay into the receiving environment.

The objective of this document is to report on the calibration and validation the OKE model and to deliver information of the connectivity characteristics around Okehampton Bay and Mercury Passage: description of observations in Section 2, description of the model, forcing and configuration in Section 3, model assessment and calibration in Section 4, and connectivity analysis in Section 5.

1.2 Background

Prior to this project, CSIRO had no calibrated local scale numerical model capable of providing connectivity information around the Okehampton Bay and Mercury Passage region. A model fit for this purpose was developed by the CSIRO Coastal Environment Modelling (CEM) team to achieve the abovementioned aim. A nested suite was required to model the Okehampton Bay region (including Mercury Passage and Spring Bay) at scales of several hundred metres. A local scale hydrodynamic model (OKE) was nested within a larger scale regional model (TASC), which in turn was nested within a global ocean model. The OKE model is described in this report; the TASC model has been developed under alternative projects.

This project has been developed through collaboration of the research team at CSIRO, the key regulators of the salmon aquaculture industry in Tasmania, the Tasmanian EPA (Environmental Protection Authority), and the environment team at Tassal, in order to ensure that the regulatory requirements are met. Additionally, the scientific value of the project is enhanced through its integration into the larger eTas information system being developed by CSIRO.

1.3 Environmental context

Okehampton Bay Marine Farming Lease 236 is located on the East Coast within the Great Oyster Bay and Mercury Passage Marine Farming Development Area (Figure 1.1). Currently the main lease holder is Spring Bay Seafoods Pty Ltd, with a portion subleased to Tassal Group Ltd. In the past, the lease was used for the farming of mussels and seaweed. Tassal received approval from the Marine Farming Planning Review Panel to farm finfish at the lease in February 2017.

Geography

Okehampton Bay is a south-facing shallow bay located on the east coast of Tasmania (Figure 1.1). The 2 km wide bay faces into Mercury Passage and is partially protected by Maria Island. The bay has some protection from northerly and prevailing westerly winds and is subject to oceanic swells from the east.

Water depths across the lease area range from approximately 20 to 28 m. The bay is bounded by Lords Bluff on the eastern side of the bay, Okehampton Beach on the northern side and Reids Beach on the western side. Beyond Lords Bluff, the next bay to the north encompasses Plain Place Beach.

Figure 0.1: Okehampton Bay and Tassal lease site.

Circulation

The eastern Tasmanian shelf lies at the boundary between two ocean currents (Ridgway, 2007) (Figure 1.2). From the north, the East Australian Current (EAC) brings relatively warm and salty nutrient-depleted sub-tropical water down the east coast of Australia to Tasmania (Pilo et al., 2015). The EAC extension consists of sporadic eddies reaching Tasmania. It peaks in February and is weakest in winter. From the south, relatively cool and fresh water from the Zeehan Current (ZC) reaches the eastern Tasmanian shelf with a peak in May-June. The ZC is an extension of the Leeuwin Current, which flows down the west coast of Tasmania, before turning around the southern tip of Tasmania.

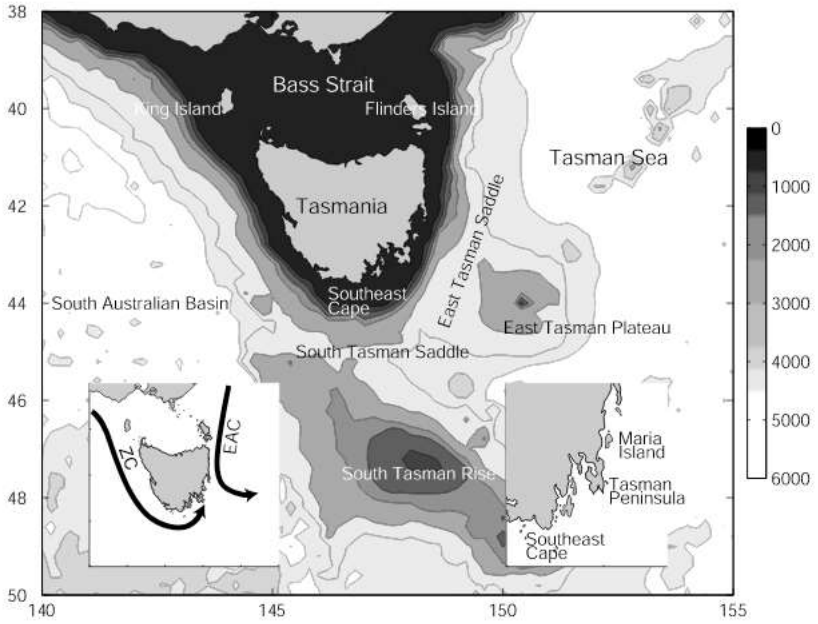

Figure 0.2: Waters around Tasmania showing both the main bathymetric features and other geographic features. The inset on the right shows the southeast coast in detail. Mercury Passage is located in between Maria Island and the east coast of Tasmania. The inset on the left shows a schematic of the major current systems in the region.

Source: Fig.1 from Ridgway et al., 2007

The strong seasonality of the EAC eddies/ZC system means that the eastern Tasmanian continental shelf is dominated by the ZC in winter, while in summer, two thirds of the shelf is dominated by the EAC eddies that opposes the ZC and pushes it to the southern part of the eastern continental shelf. Autumn and spring are periods of transition between these two states (Oliver et al., 2016).

Both long-term trends and variability in upper ocean temperatures are large along the east coast of Tasmania, with sea surface temperature warming 3–4 times more than the global average rate. Long-term trends are attributed to increased intensity of the EAC extension (Ridgway, 2007; Sloyan & O'Kane, 2015). These trends are particularly strong in autumn, indicating a lengthening of the warm season (Oliver et al., 2018).

The EAC is the dominant driver of marine heatwaves across the eastern and southern part of Tasmania, with strong EAC years related to significantly more summertime marine heat wave days (Oliver et al., 2016, 2018). In summer 2015/2016, the Tasman Sea experienced its longest and most intense marine heatwave ever recorded. Since then, the 2016/2017 and 2017/2018 summers have exhibited intense marine heat waves.

2. Observations

Calibration of hydrodynamic models is best served through assessment against high frequency conservative variables, such as sea level, salinity or temperature. It is useful to augment this with less conservative variables (e.g. velocity) or high spatial resolution snapshot datasets. A data record that captures seasonality is required, so at least an annual cycle is useful, or at a minimum winter and summer seasonal records. A summary of locations of available observations is provided in Figure 2.1.

Figure 0.3: Location of the observations used for calibration and validation.

2.1 Historical dataset

For sea level, we have used the sea level records from the Spring Bay tide gauge. For temperature and salinity, Tassal provided historical data from temperature loggers and DO (dissolved oxygen) buoy. These datasets are described below.

Temperature loggers from Marine Solutions were located in the Okehampton Bay lease from 31 Oct 2014 until 28 June 2017 (pinned as "loggers" in Figure 2.1) and these provided hourly temperature records at 4 depths: 3, 10, 20 and 25 m. Temperature and salinity sensors on a DO Buoy located inside the lease also provided 15-minutes record at 2 depths (3 and 10 m) from 23 January until 1 September 2017 for temperature, and from 6 April 2017 until 1 September 2017 for salinity. This buoy was operated by Xylem & is pinned as "DO buoy" in Figure 2.1.

Paddy's Point data loggers provided temperature and salinity at 3 depths (1m/surface, 5m and 1m above sea bed) from 21 June 2018 until 18 July 2018. It was operated by Marine Solutions and is pinned as "Paddys" in Figure 2.1.

The ongoing far-field ambient monitoring program consists of seven Broadscale Environmental Monitoring (BEMP) sites, where bi-monthly sampling of temperature and salinity are performed at 3 depths : surface, 5m, and 1m off the seabed (performed once a month by Tassal (Aquenal) and once a month by EPA). From August 2014 until August 2017, 5 sites were monitored (Spring Bay, Okehampton Bay, North Mercury

Passage, North Maria, Central Mercury Passage), and from September 2017 until July 2018, 7 sites were monitored (addition to Cape Bougainville, South-of-Lease). Table 2.1 provides details of the BEMP sites.

Table 0.1: Details of sites in the Okehampton Broadscale Environmental Monitoring Program.

Site ID/Name	Location	Easting	Northing	Distance from Lease	1m off the seabed (m)
BEMP-MP1	Spring Bay	575137	5288199	Far-field	14.7
BEMP-MP2	Okehampton Bay[1]	580316	5291659	Local	20.5
BEMP-MP3	North Mercury Passage	584357	5290660	Far-field	45.0
BEMP-MP4	North Maria	586953	5287632	Far-field	28.9
BEMP-MP5	Central Mercury Passage	580785	5281866	Far-field	27.1
BEMP-MP6	Cape Bougainville[2]	583513	5292985	Far-field	30.6
BEMP-MP7	South of Lease[3]	579367	5290031	Intermediate	23.8

1 Compliance site; control site.

2 Note that the sampling location for MP6 since September 2017 was ~200 m from the coordinates set out in the EPA licence. For data consistency these coordinates will be maintained for future sampling.

3 Note that the sampling location for MP7 between September 2017 and April 2018 was ~200 m to the north of the coordinates set out in the EPA licence. Since this site is co-located with video and benthic sample sites, sampling was adjusted in the May 2017 survey to align with the EPA licence

The coordinate for MP7 is the one sampled since May 2018. Between September 2017 and April 2018 the MP7 sampling point was 200 m north (coordinates 55 G 579480 5290216)

The above historical dataset was not deemed optimum for calibration purposes as it did not contain continuous records of sufficient length (seasonal cycles) with adequate spatial variability. This is particularly true of salinity, which being the most conservative tracer that may be potentially observed (although can be difficult to continuously measure), is valuable for calibration purposes. A targeted observation program was therefore considered necessary.

2.2 The 2018-2019 dataset

As in-kind contributions to this project, Tassal contracted local marine consultancy business, Marine Solutions, to deploy three moorings within the local region to host surface, mid-water column and bottom instruments, collecting temperature and salinity at high frequency (sites 1 to 3 in Figure 2.1). 21 HOBO DO loggers measured temperature and DO throughout the water column, allowing for some replicate measurements at 8 depths. 9 HOBO salinity loggers measured salinity and temperature at the surface, middle and bottom at all 3 sites. Two EXO3 units were also added from April 2019 at the surface of sites 1 and 3, to measure potential low-salinity plumes.

Temperature data from the HOBO DO loggers have been recovered for the period of September 2018 to end of July 2019. Unfortunately, although the HOBO salinity loggers provided some usable salinity data, failures in these loggers resulted in this overall salinity dataset to be deemed too segmented and unreliable (see discussion in section 4.2). However, the 9 HOBO salinity loggers also had temperature sensors, allowing for some extra temperature comparisons from April 2019 to August 2019. This combined temperature dataset is the one used for calibration of the model.

Furthermore, due to some uncertainty around the trend over a 3-month period, and the absence of synoptic events during the observation period, the EXO3 dataset was also not used for calibration (see discussion in section 4.2).

Site 1: Corner of Spring Bay Seafood lease

32 m depth, 8 DO loggers, 3 salinity loggers, 1 EXO3 unit

- Surface= DO logger, DO logger (replicate), salinity logger, EXO3 unit
- 5 m= DO logger, DO logger (replicate)
- 10 m= DO logger
- 15m= Salinity logger
- 20 m= DO logger
- Bottom (31 m)= DO logger, DO logger (replicate), salinity logger

Site 2: SE corner marker of Tassal Okehampton lease

28 m depth, 8 DO loggers, 3 salinity loggers

- Surface= DO logger, DO logger (replicate), salinity logger
- 5 m= DO logger, DO logger (replicate)
- 10 m= DO logger
- 15m= Salinity logger
- 20 m= DO logger
- Bottom (27 m)= DO logger, DO logger (replicate), salinity logger

Site 3: Southern Wood Chip Dolphin Wharf

12 m depth, 5 DO loggers, 3 salinity loggers, 1 EXO3 unit

- Surface= DO logger, DO logger (replicate), salinity logger, EXO3 unit
- 5 m= DO logger, DO logger (replicate), salinity logger
- Bottom (11 m)= DO logger, salinity logger

3. The hydrodynamic model

3.1 Sparse Hydrodynamic Ocean Code

The hydrodynamic model SHOC (Sparse Hydrodynamic Ocean Code; Herzfeld et al., 2006, https://research.csiro.au/cem/software/ems/hydro/strucutured-shoc/) is employed for this study. SHOC is the hydrodynamic component of the broader Environmental Modelling Suite (EMS), which includes libraries for sediment transport, biogeochemistry (BGC), waves and tracer statistics (https://research.csiro.au/cem/software/ems/). SHOC is a general-purpose model based on the paper of Blumberg and Herring (1987), applicable on spatial scales ranging from estuaries to regional ocean domains. It is a three-dimensional finite-difference hydrodynamic model, based on the primitive equations. Outputs from the model include three-dimensional distributions of velocity, temperature, salinity, density, passive tracers, mixing coefficients and sea level. Inputs required by the model include forcing due to wind, atmospheric pressure gradients, surface heat and water fluxes and open-boundary conditions such as tides and low frequency ocean currents (Figure 3.1). The model is based on the equations of momentum, continuity and conservation of heat and salt, employing the hydrostatic and Boussinesq assumptions. The equations of motion are discredited on a finite difference stencil corresponding to the Arakawa C grid.

The model uses a curvilinear orthogonal grid in the horizontal and a choice of fixed ‘z’ coordinates or terrain-following σ coordinates in the vertical. The ‘z’ vertical system allows for wetting and drying of surface cells, useful for modelling regions such as tidal flats where large areas are periodically dry. The current implementation of the model uses z-coordinates. The bottom topography is represented using partial cells. SHOC has a free surface and uses mode splitting to separate the two-dimensional (2D) mode

from the three-dimensional (3D) mode. This allows fast moving gravity waves to be solved independently from the slower moving internal waves allowing the 2D and 3D modes to operate on different time-steps, resulting in a considerable contribution to computational efficiency. The model uses explicit time-stepping throughout except for the vertical diffusion scheme which is implicit. A Laplacian diffusion scheme is employed in the horizontal on geopotential surfaces. Smagorinsky mixing coefficients may be utilized in the horizontal. The ocean model can invoke several turbulence closure schemes, including k-ε, k-ω, Mellor-Yamada 2.0 & 2.5 and Csanady type parameterizations. A variety of advection schemes may be used on tracers and 1st or 2nd order can be used for momentum. The model also contains a suite of open boundary conditions, including radiation, extrapolation, sponge and direct data-forcing. A generous suite of diagnostics is included in the model.

The 'sparse' coordinate system (Herzfeld, 2006) employed by SHOC facilitates the use of highly complex curvilinear grids that allow resolution optimization. This sparse system allows the removal of dry land cells in the gridded domain, thus reducing the computational burden. It has been shown that runtime increases exponentially as wet cell ratios decrease using the sparse system (Herzfeld, 2006). The sparse system also presents several other advantages, including arbitrary domain decomposition for distributed processing, reduced file sizes for storage and compatibility with finite volume approaches.

Detailed Science and User Manuals for SHOC can be downloaded from https://research.csiro.au/cem/software/ems/ems-documentation/.

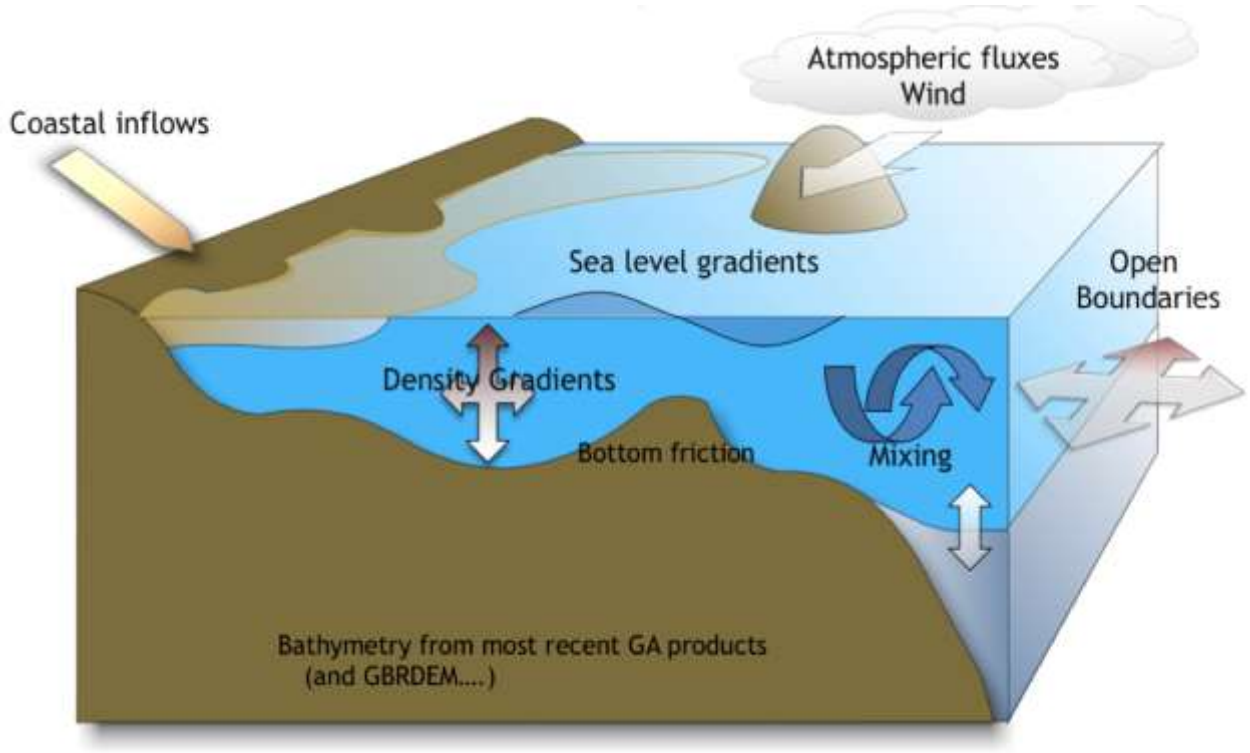

Figure 0.4: Schematic representation of major forcing inputs for the SHOC hydrodynamic model.

3.2 Nested suite of hydrodynamic models

The grid configuration

In order to achieve a level of resolution in the order of hundreds of meters in Okehampton Bay (Figure 3.2), a downscaling strategy was required, where models of increasing resolution are nested within each other until the target resolution is achieved. There are limitations as to the amount of resolution that can be increased across nesting boundaries, with a rule of thumb that 5:1 is an acceptable upper bound. It is standard practice to nest regional applications within global ocean models (e.g. OceanMAPS, http://wp.csiro.au/bluelink/global/oceanmaps/) so that all modes of forcing are introduced into the target domain. In order to satisfy the above-mentioned nesting ratio, a nested suite of 2 downscaled models was required for Okehampton Bay and Mercury Passage.

The regional nested model is the CSIRO South-East Australia Regional Model, developed under the CSIRO eTas Information System. The current CSIRO South-East Australia Regional Model is TASC (Figure 3.3). The nested higher resolution model of Okehampton Bay and Mercury Passage (OKE, Figure 3.2) was developed for this project using the CSIRO Environmental Modelling Suite (https://research.csiro.au/cem/software/ems/), using the SHOC hydrodynamic model (https://research.csiro.au/cem/software/ems/hydro/strucutured-shoc/).

The OKE model grid is curvilinear with 200 x 130 = 26000 horizontal grid cells (Figure 3.2). A quasi-polar configuration is utilized where resolution increases away from the boundary, with grid resolution ranging from around 400 m on the offshore boundary (1/5 of the TASC resolution of 2km), to around 100m near the lease in Okehampton Bay, and no more than 280 m in the passage between Okehampton Bay and Maria Island. The resolution in the neighbouring bays is around 100m along Plain Place Beach to the north,

150m near Triabunna and Spring Bay, 200m near Orford and 250m near Darlington Harbour on Maria Island.

The water depth over the model domain ranges from 0 to 85 m, however for stability reasons, a depth minimum of 1 m has been imposed for all model runs. There are 28 model layers in the vertical and the model 3D time step is 20 seconds.

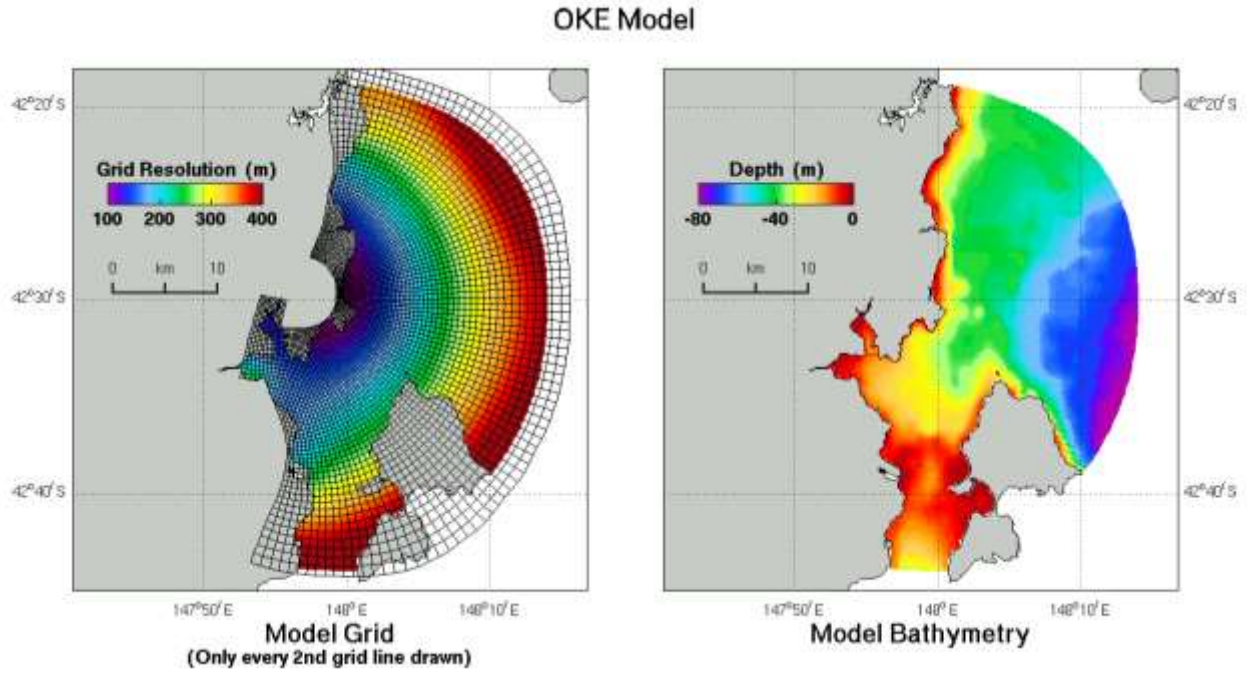

Figure 0.5: OKE model domain: grid configuration (left) and bathymetry (right).

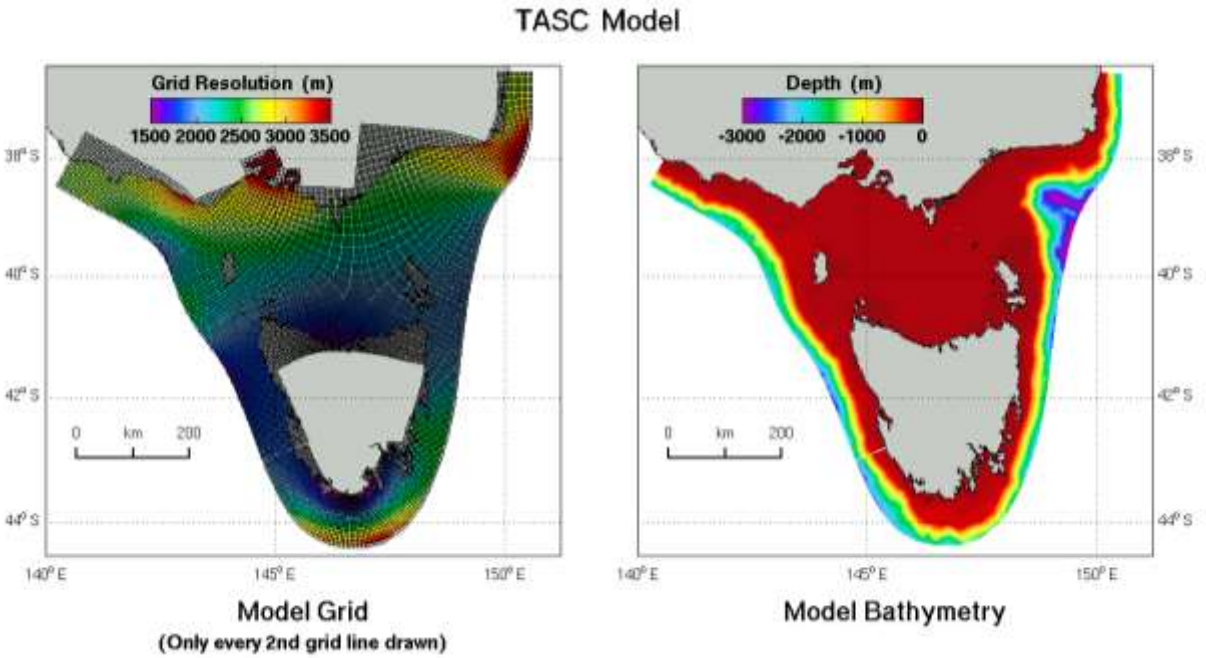

Figure 0.6: TASC model domain: grid configuration (left) and bathymetry (right).

Bathymetry

Two datasets have been used to construct the OKE grid bathymetry, as depicted in Figure 3.4:

- high resolution data around the sites of interest was provided by Tassal
- coarse 1km gridded data for the far-field was derived from Geoscience Australia (2002).

There are more recent and higher resolution bathymetry data sets available from Geoscience Australia (GA), however, these datasets exhibit more discontinuities in coverage in and around Spring Bay, hence the 2002 dataset was used in preference.

Overall, the bathymetry data we have used could be described as fair. Although there were some discrepancies of a few metres between observed BEMP station depths and the corresponding model depths, the data was still deemed as satisfactory.

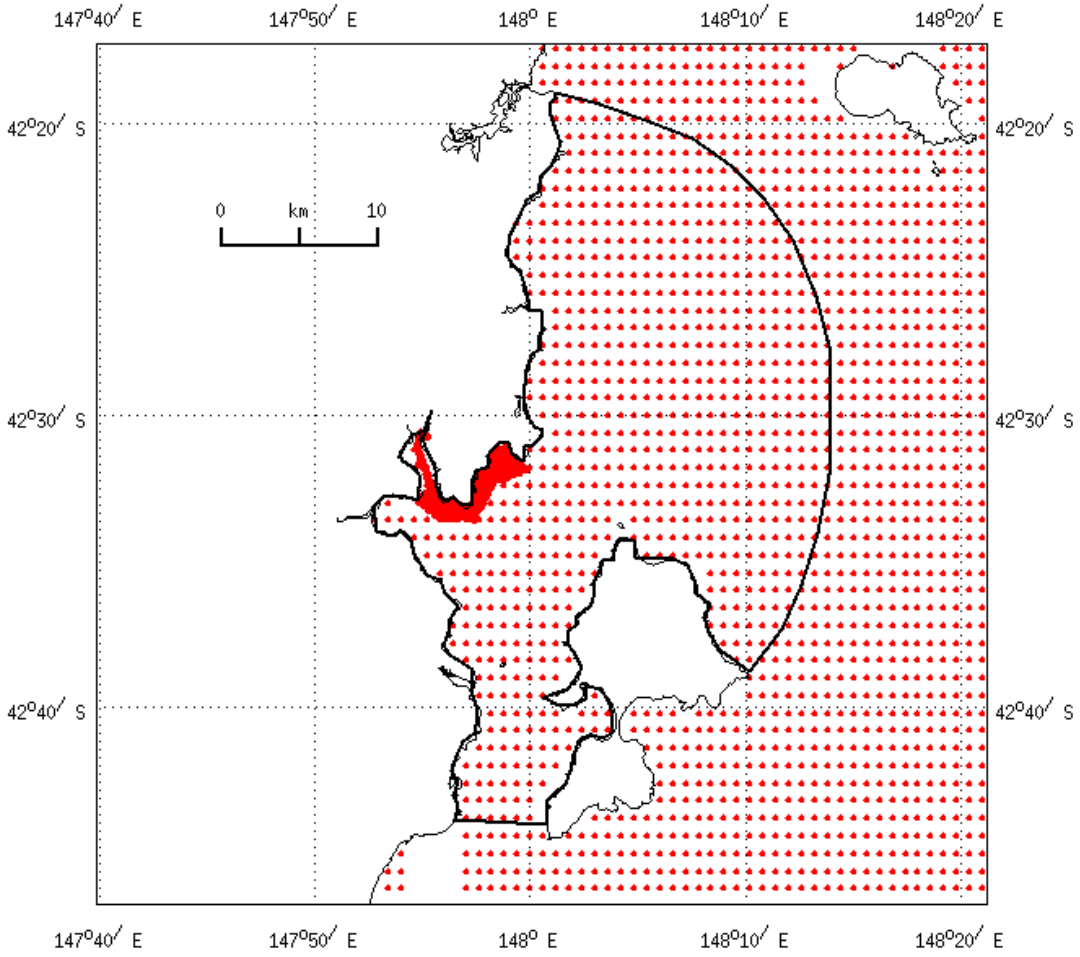

Figure 0.7: 2 Bathymetry datasets used for the OKE grid.

3.3 Forcing and initial conditions

The ocean boundary forcing consists of daily fields of three-dimensional velocities, sea level, temperature and salinity. For TASC, open ocean boundary forcing and initial conditions were from the global OceanMAPS model, operated by Bureau of Meteorology (http://www.bom.gov.au/oceanography/forecasts/site-help.shtml) while OKE uses output from TASC for open boundary information.

Surface atmospheric fluxes (momentum, heat and freshwater) at 3-hour intervals were provided by the Bureau of Meteorology's ACCESS-R atmospheric model with a resolution of ~12 km (http://www.bom.gov.au/australia/charts/about/about_access.shtml).

Runoff from the Prosser River is included in the OKE model by specifying the flow rate and temperature of freshwater input. The flow rate is provided by DPIPWE, but as the gauge is located above a small water storage dam, the flow rate does not necessarily accurately represent the flow into the ocean at all times, especially during low flow. The forcing data used in the OKE model is summarized in Table 3.1.

Table 0.2: Data requirements for the OKE hydrodynamic model

Forcing	Data	Source
OKE		
Open boundary conditions	TASC	CSIRO
Initial conditions	TASC	CSIRO
Meteorological surface fluxes	ACCESS-R	BoM
River flow	Gauged	DPIPWE
TASC		
Open boundary conditions	OFAM(OceanMAPS)	BoM
Initial conditions	OFAM (OceanMAPS)	BoM
Meteorological surface fluxes	ACCESS-R	BoM
River flow	Gauged	DPIPWE

3.4 Configuration summary and Simulations

The OKE model runs in both hindcast and near-real time modes, predicting three-dimensional fields of temperature, salinity and currents in Okehampton Bay and environs. The model runs at approximately 120 x real-time using 16 processors (i.e. a 1-year simulation takes approx. 3 days to complete). Key model parameters are summarized in Table 3.2.

Table 0.3: Key parameters for the OKE hydrodynamic model.

Parameter	Value
Grid size	200 x 130
# layers	28
Turbulence closure	k-□ (Burchard et al., 1998)
Background vertical viscosity	$1x10^{-7}$ m^2s^{-1}
Background vertical diffusivity	$1x10^{-7}$ m^2s^{-1}
Background horizontal viscosity	10 m^2s^{-1}
Horizontal diffusivity & viscosity	Smagorinsky, (1963) c=0.1
Horizontal advection	ULTIMATE QUICKEST (Leonard, 1991)
Time steps (3D/2D)	20 / 2 s
Bulk scheme	Kitiagorodskii et al (1973)

Short wave attenuation	0.1 m^{-1}
Short wave transmission	0.8
Short wave bottom absorption	0.5
Open boundary scheme	Herzfeld & Andrewartha (2012)
Boundary relaxation timescale	3 seconds

The pilot run for OKE covered the January 2016 to December 2017 period (Langlais et al., 2019).

As mentioned above, calibration of hydrodynamic models is best served through assessment against high frequency conservative variables, such as sea level, salinity or temperature. A data record that captures seasonality is required, so at least an annual cycle is useful, or at a minimum, winter and summer seasonal records. Making use of the 3 moorings deployed from November 2018 to end of July 2019, the calibration period was set from 02/08/2018 to 01/08/2019. The same period was used to assess the connectivity around Okehampton Bay and Mercury Passage.

4. Model calibration and assessment

In this section, the performance of the hydrodynamic model is quantitatively assessed against in-situ observations of temperature, salinity and sea level.

4.1 Methodology

The hydrodynamic model is to be ultimately used to predict the fate of passive tracers. These tracers are governed by the conservation equation, and for a conservative substance, with no sources or sinks, the concentration distribution is determined by advection and diffusive processes. If the model is correctly predicting a passive tracer distribution, then this implies the underlying velocity distribution and mixing regime is also correct. Consequently, the aim is to calibrate the model against available passive tracers, e.g. temperature and salinity. While these tracers are not entirely passive, the major sources and sinks (surface fluxes for heat and freshwater inflows for salt) can be well quantified, hence if the behaviour of these variables correlates well with observations we have confidence the underlying transport fields are correct in the model and the model is fit for purpose to predict the fate of introduced passive tracers.

The observational record of salinity revealed some issues (see discussion in section 4.2), hence the calibration was solely based on the temperature field (section 4.3). Although salinity is considered more passive than temperature, if the surface fluxes are well quantified then temperature can also provide equivalent confidence. In order for both temperature and salinity to be useful for calibration, these observational records are required to possess some variability (e.g. impacts of flood plumes). In this case study, the lack of freshwater inputs during the observational period meant that such variability was largely absent for salinity, thus limiting its potential usefulness. Comparison of the model sea-level with sea-level measured at Spring Bay provides estimates of model skill at tidal and low frequencies (section 4.4). In section 4.5, a specific event is analysed: seasonal and synoptic variability of temperature and salinity can be linked with known dynamical processes (flood plumes, upwellings, intrusions of offshore water) and inform us on the performance of the model in representing the complex circulation in Mercury Passage.

Throughout this section, we use 5 skill metrics: the root-mean-square error (RMSE), the mean absolute error (MAE), correlation coefficient (cc), model bias, and model skill (d2) described by Willmott et al. (1985).

Model bias assesses whether the simulated variables are under-or over-predicting observed values. The RMSE and MAE are a measure of the absolute magnitude of the "error" averaged over the time-series. A RMSE or MAE of 0 indicates a perfect fit. The Willmott model skill is designed to quantify errors that are unevenly distributed in time or space. It weights the model errors relative to the known amplitude of local variability.

The Willmott index is computed as the difference between the model and observation anomalies relative to the time-average observations, divided by the sum of observed anomalies relative to the time-average observations. It varies between 0 and 1. A value of 1 indicates a perfect match, and 0 indicates no agreement. For physical parameters such as salinity and temperature and high spatial and temporal observations, a Willmott skill above 0.7 demonstrates a good agreement between model and observations.

4.2 Salinity

Salinity observations were retrieved from a DO buoy at the lease site from 6 April 2017 until 1 September 2017, and at the 3 mooring sites from April 2019 to June 2019. Unfortunately, none of these observations provided usable datasets (Figure 4.1).

When comparing surface salinity from the 3 sites with surface observations from the Maria Island IMOS mooring (which gives information about offshore waters) and with OceanMaps (the BoM ocean forecast model extracted at Maria Island mooring location), the time-averaged observations appear too salty at the 3 sites, displaying unrealistic salinity exceeding 36 (Figure 4.1 top panel). The time variability is also unrealistic, with standard deviations exceeding 0.5. There are also some erroneous diurnal variations in the salinity timeseries. Throughout the data collection process, various mitigation attempts (e.g. increases in maintenance and cleaning frequencies) were implemented to aid in addressing these observed discrepancies. However, as previously mentioned, although the salinity loggers did provide some usable salinity data, overall the salinity dataset was deemed too segmented and unreliable to be of use. Even so, there were no significant variations in salinity (e.g. flood plumes) in the data collection period for salinity to make a valuable contribution to model calibration.

While the mean salinity magnitude measured by the DO buoy is more realistic, the time variability is too large (Figure 4.1 bottom panel), and the values of ~34 in Okehampton Bay appear too low in the absence of freshwater input. It would take a very large flood from a relatively small river like the Prosser for salinity to be impacted to such a degree in Okehampton Bay.

EXO3 sensors were also deployed at the surface at Site 1 and 3; compared to the HOBO salinity logger data, the EXO3 shows much less variability (Figure 4.2). There is, however, a trend (or drift) with salinity that starts ~1 psu saltier than the model in May 2019 and decreases to ~0.2 psu saltier in late July 2019. The relatively short duration of this data (3-month) combined with the absence of additional data for cross-referencing purposes makes it difficult to discern if this decrease in salinity is a real signal (e.g. seasonal variability) or an unrealistic drift in the sensor. Apart from this freshening trend, there is very little variability, with no freshwater plume events which could have been used for calibration. Due to the uncertainty around the trend over a 3-month period, and the absence of synoptic events during the observation period, the EXO3 dataset was also not used for calibration.

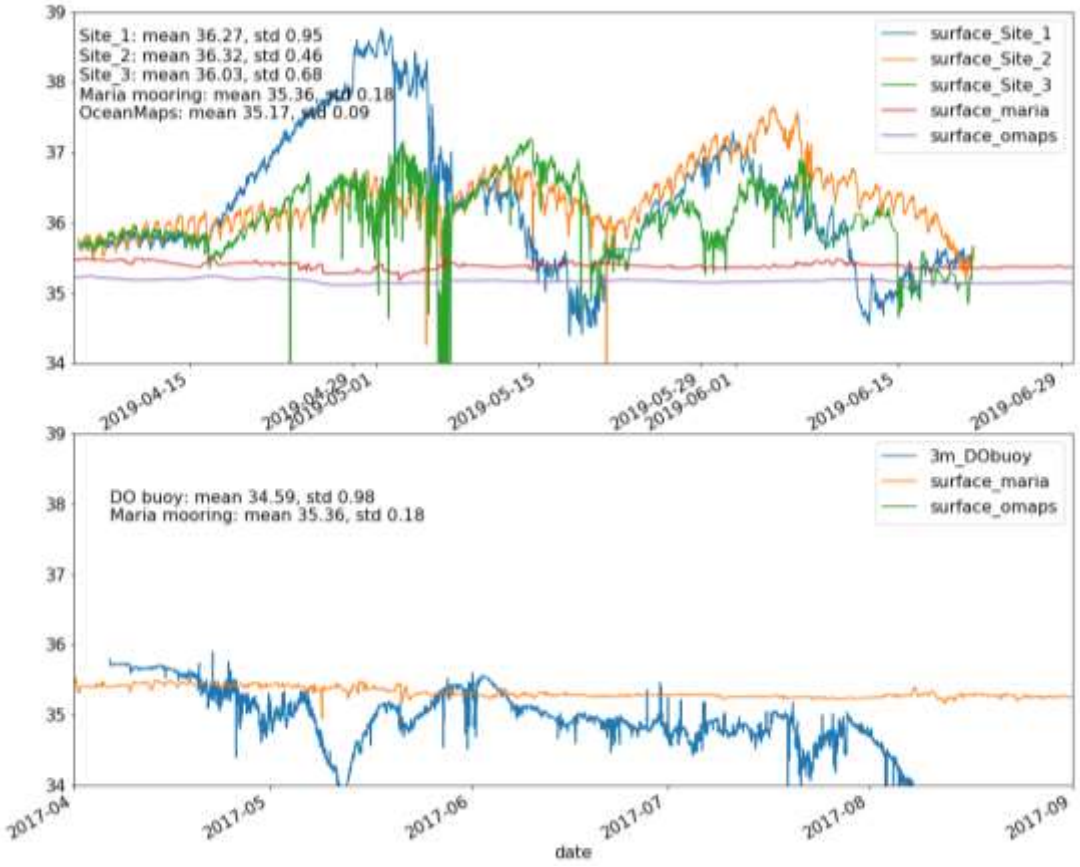

Figure 0.8: Comparison between salinity observations, the salinity from Maria Island IMOS mooring (situated east of Maria Island) and OceanMaps salinity (the BoM ocean forecast model extracted at Maria Island mooring location) for 2 periods: from April 2019 to June 2019 (top panel) and from April 2017 until September 2017 (bottom panel).

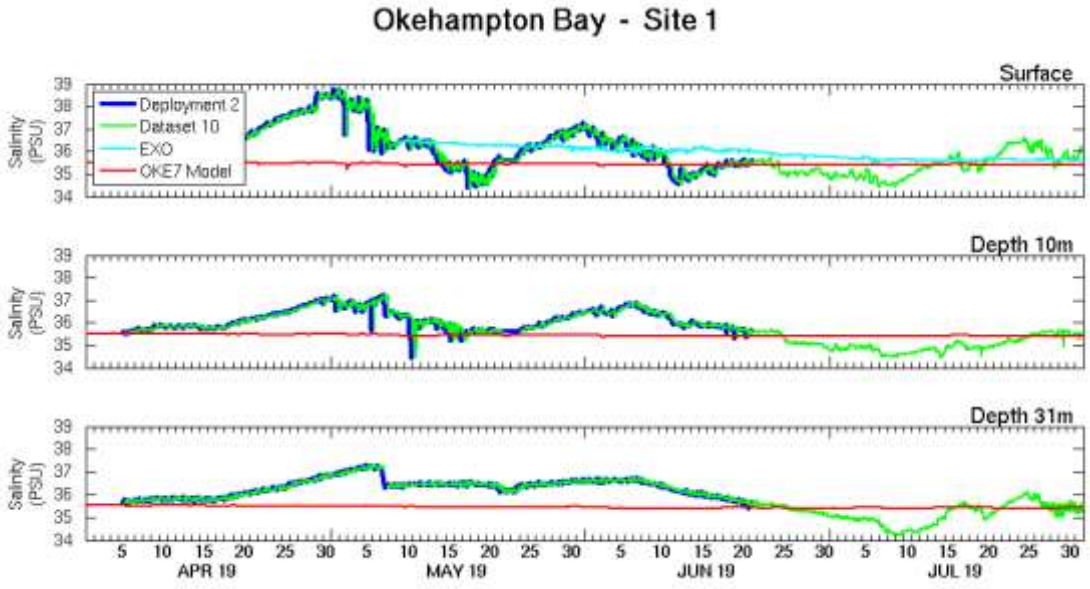

Figure 0.9: Comparison of salinity observations at Site 1.

Limited impact for the calibration

Salinity has sources and sinks through the surface from evaporation and rainfall, and from river inflow. In coastal areas like Okehampton Bay, salinity may vary seasonally due to air-sea fluxes and episodically due to flood events. The observational record of a flood plume, where salinity rapidly drops then recovers slowly to marine levels, would have provided an excellent event to which model salinity could be calibrated. However, we note that during the period August 2018-2019 there were no significant outflows from the Prosser River, except for a 40 cumec spike in late November 2018 (Figure 4.3). The Prosser flow is measured above a dam and due to the very dry conditions before the event, it is likely that this spike in the flow was stored within the dam with very little overflowing into the ocean. As a consequence, there were probably no flood plumes suitable for model calibration in 2018-2019. Hence, the absence of a good salinity record does not degrade the model calibration in this case. If such a record could be acquired and assessed against in the future, the confidence in model predictions would then be anticipated to further increase.

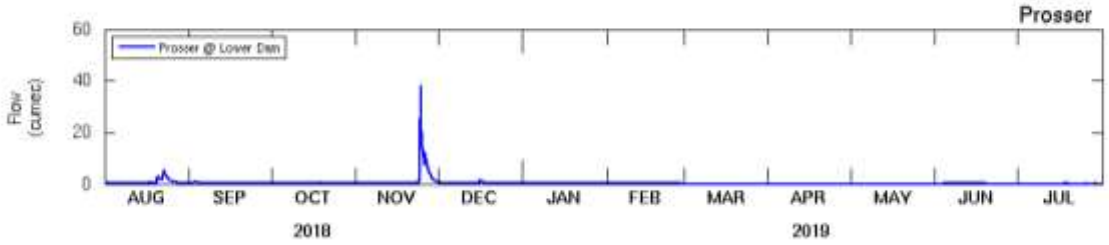

Figure 0.10: Time series of the Prosser River flow upstream of the dam for the 2018-2019 modelling period.

Bias correction of OceanMaps

OceanMaps shows a clear bias of 0.2 psu at the Maria Island IMOS mooring (Figure 4.1 top panel). A correction has been applied at the open ocean boundaries of the regional TASC model to take this bias into account. As TASC provides the open ocean boundary conditions for the OKE model, this correction propagates into the OKE model.

4.3 Calibration

Parameters

Due to the salinity data issues and lack of variations in salinity (e.g. flood plumes), the calibration was solely based on temperature and elevation data for the 02/08/2018 to 01/08/2019 period, when high temporal coverage data was available at the 3 mooring sites. The temperature has large sources and sinks through the surface from atmospheric heat fluxes. The calibratable parameters relating to the input of heat at the surface and the vertical distribution of heat were optimized against observations. We repeatedly ran the model over the 02/08/2018 to 01/08 2019 period, until errors between the model predictions and the temperature measurement at the 3 sites were minimised.

Specifically, we modified the following parameters:

- the Bulk scheme impacting the heat fluxes,

- the Short Wave Radiation (SWR) parameters impacting the penetration of heat at depth,
- the vertical turbulent closure impacting the vertical mixing in the water column and the redistribution of heat in the water column.

Observation uncertainties

The replicate temperature loggers at the surface and at depth allowed for continuous measurements when loggers failed and allowed for evaluation of uncertainties in the observations when simultaneous measurements were made. The RMSE achieved between the DO-Temperature loggers, is 0.04 and 0.12 ^{o}C, with biases smaller than 0.12 ^{o}C. The RMSE achieved between DO-temperature logger and the Conductivity-Temperature logger is slightly higher, reaching 0.5 ^{o}C occasionally.

Results

To demonstrate the impact of the calibration, the different skill metrics are presented for the initial pilot model and the calibrated model.

The comparison between the temperature observations at the 3 sites and the pilot model were already quite good, with Willmot skill scores between 0.87 and 0.9. The pilot model shows an overall cold bias that increases with depth: with a bias of -0.21 to -0.37 ^{o}C in the first 10 m and a bias of -0.35 to -0.50 ^{o}C below 20 m deep. The pilot model shows some RMSE of 0.41 to 0.52 ^{o}C between the surface and 10m deep, and larger RMSE of 0.54 to 0.65 ^{o}C below 20m deep.

To reduce the cold bias, the calibration parameters were modified to enhance the heat flux at the air-sea interface. To reduce the RMSE in the bottom layers, the parameters were modified to enhance the penetration of heat at depth. It resulted in a calibrated model with Willmot skill scores above 0.9 (between 0.91 and 0.94) RMSE smaller than 0.4^{o}C throughout the water column and small biases between -0.01 and +0.17 ^{o}C (Figures 4.4 to 4.6). The biases fall within the uncertainty of the observations and give high confidence in the calibration of the model.

The seasonal and synoptic responses are well captured by the calibrated model (Figures 4.4 to 4.6). The synoptic scale temperature oscillations are particularly strong in summer and winter and are characterized by warming and cooling events in the different ocean layers. The model captures the timing of these events well. The amplitude of the cooling or warming events is also well captured by the model (see section 4.5 for a detailed analysis), even though it is occasionally a little too weak. For example, at the end of October 2018 a warming event occur in the surface layers and is captured by Sites 1, 2 and 3. The model shows a cold bias of 0.3^{o}C during this event. The model is also a little too warm at the end of February at Site 1.

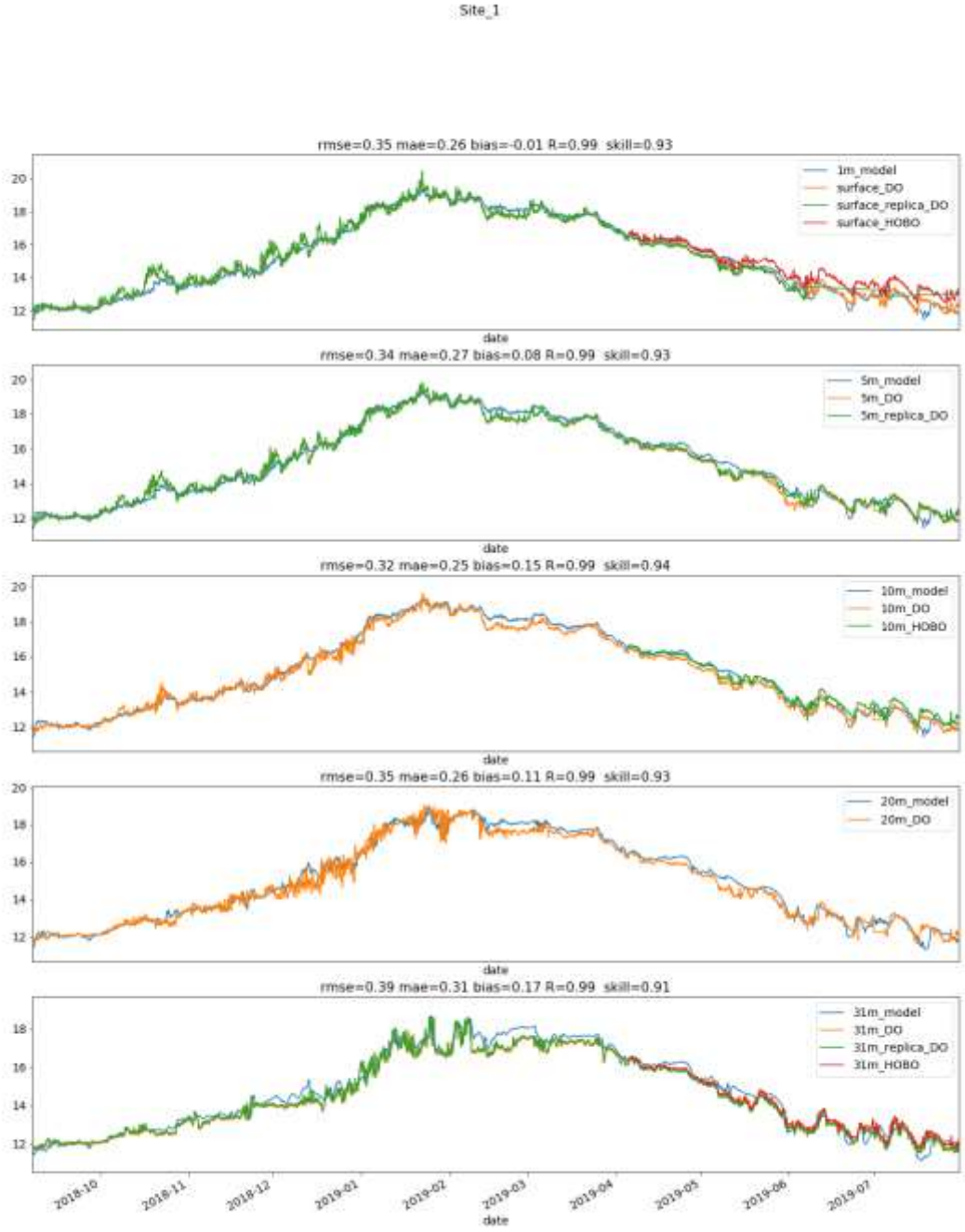

Figure 0.11: Temperature comparison between the observations and the calibrated model at the Site 1, Corner of Spring Bay Seafood's lease in Mercury Passage, for 4 depths: surface, 5m, 10m, 20m and 31m (from top to bottom).

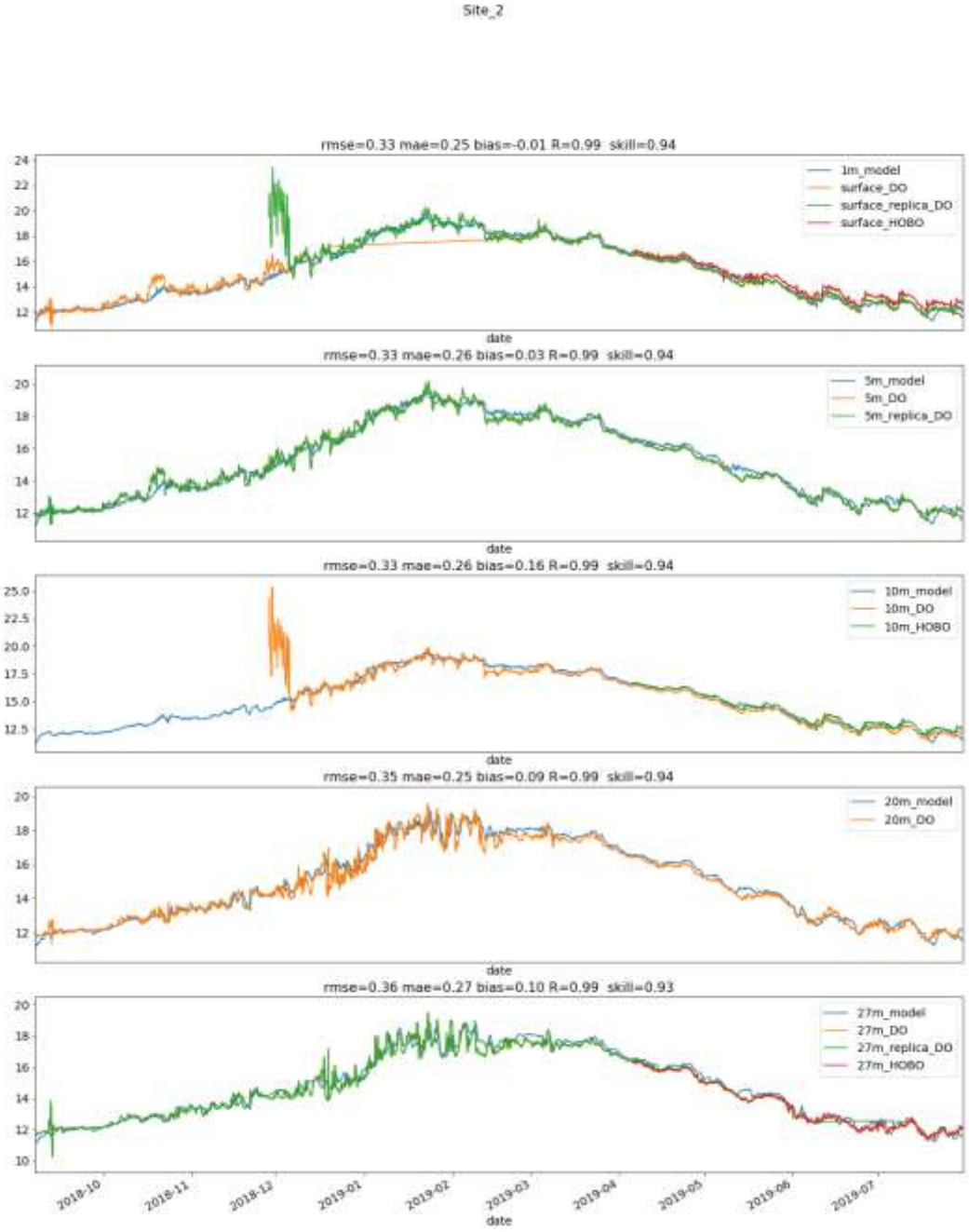

Figure 0.12: Temperature comparison between the observations and the calibrated model at the Site 2, SE corner marker of Tassal Okehampton Bay Lease, for 4 depths: surface, 5m, 10m, 20m and 27m (from top to bottom).

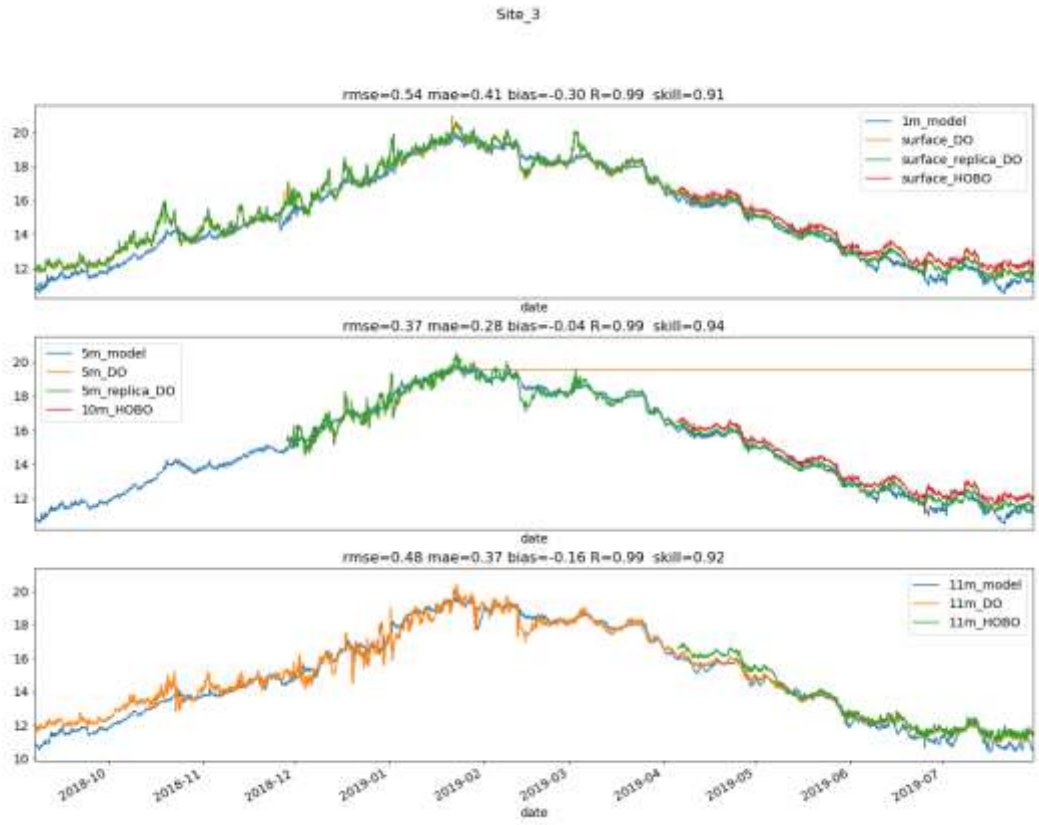

Figure 0.13: Temperature comparison between the observations and the calibrated model at the Site 3, at the Southern wood chip dolphin wharf, for three depths: surface, 5m and 11m (from top to bottom).

4.4 Sea level

We validate the model against sea level measured at Spring Bay (Figures 4.7 and 4.8). The skill metrics were computed for the total signal and low frequencies over the full-year August 2018-July 2019 (Figure 4.7). The latter is of most importance here, as this determines the long term barotropic fate of material. For visualisation purposes, a 6-day period is also shown, to allow us to clearly observe whether the model is accurately capturing the key characteristics of tidal amplitude, phase and form factor (Figure 4.8).

The OKE model shows good skill at tidal and low frequencies. The model tidal magnitude and phase compares very well to observation (RMSE = 0.07 m, MAE = 0.05 m, bias = 0.0009 m), the tide is in phase with observation (cc = 0.98) and overall the model exhibits very high skill (d2=0.99). The neap-spring cycle is also well resolved. Skill metrics for the low frequency component also show good skill (RMSE = 0.03 m, MAE = 0.02 m, cc = 0.97, bias = 0.001 m and d2=0.98). It is important to note that skill is slightly degraded occasionally, with some smaller amplitude of the model in the low frequency for short periods of time (Figure 4.7 bottom panel).

Overall, the comparison of the model with sea level measurements indicates a good tidal forcing at the open boundary and a good propagation of the tidal signal inside the model, which reflects an adequate representation of the bathymetry. Low frequency motion is also well represented - again this is an important result since it is the low frequency response of the domain that dictates the residual circulation and hence long-term fate of passive contaminants.

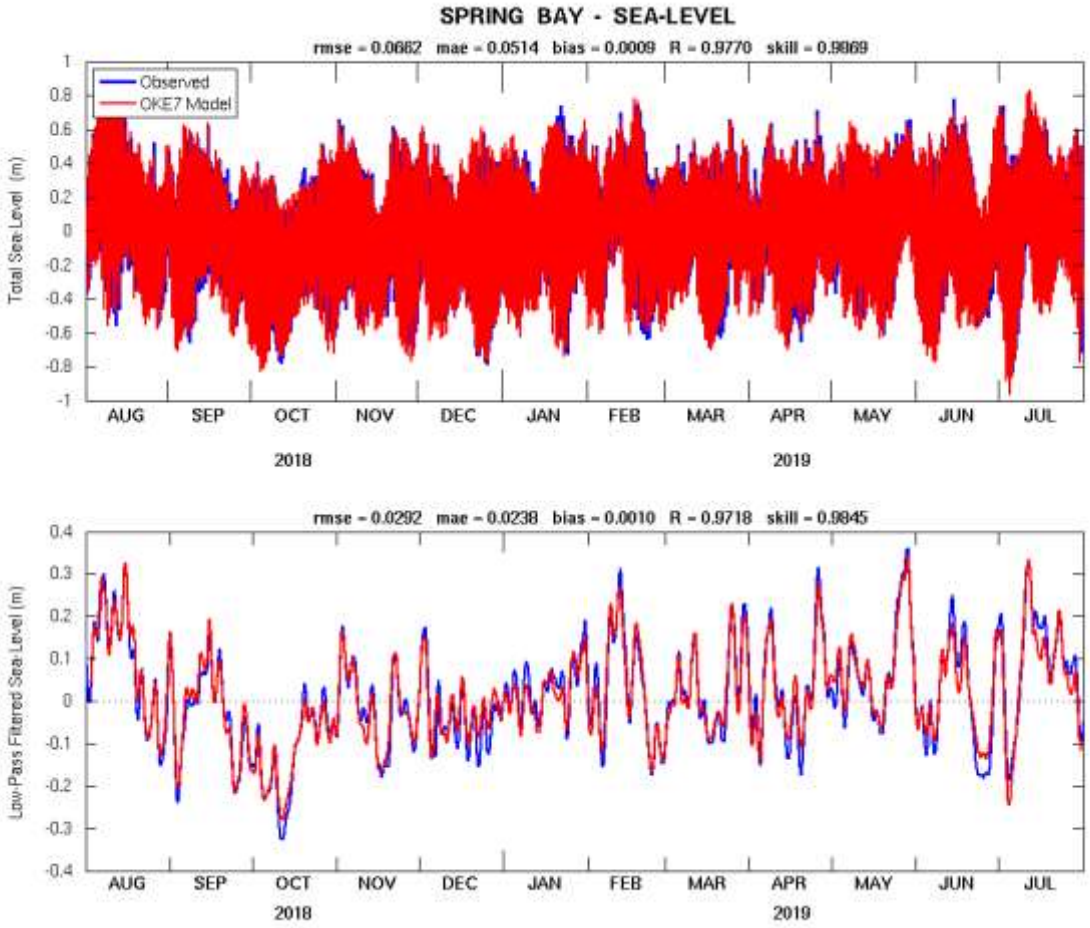

Figure 0.14: Tidal sea level (top) and low-pass filtered sea level (bottom) at Spring Bay for August 2018 to July 2019.

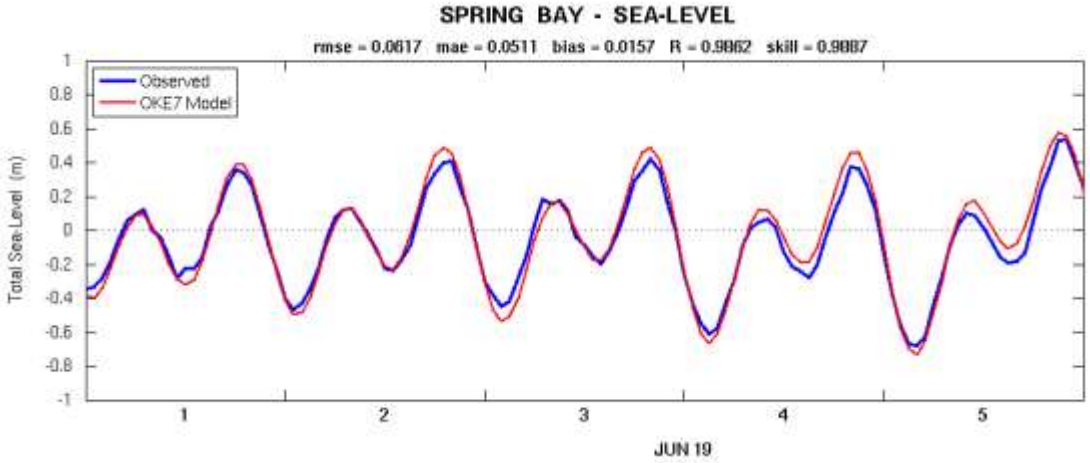

Figure 0.15: Tidal sea level at Spring Bay for June 2019.

4.5 Intrusions

In this section, we link some synoptic variability of temperature at the mooring sites with dynamical processes. We focus on a synoptic warming event in October 2018 and some repetitive cooling/warming events in June and July 2019.

Warming event

From October 15th to October 30th 2018, a 1.5-2^{o}C warming event occurs at the 3 mooring sites in the first 10m of water (Figure 4.9). This event is well captured by the OKE model, although the amplitude of the warm anomaly is a little too weak in the model (a 1^{o}C anomaly is modelled). Looking at the evolution of the surface temperature and depth-average circulation over this period (Figure 4.10), we observe a switch between a southward to a northward flow in Mercury Passage on the 15th of October. The northward flow is entering the domain through the southern open boundary and brings warm water into the domain. Moreover, the northward flow entrains warm water formed in the shallow Shoal Bay on Maria, enhancing the warm signal. The good representation of this warm intrusion through the southern boundary gives us good confidence in the performance of the model in capturing the transport of water masses correctly and representing the complex circulation in Mercury Passage.

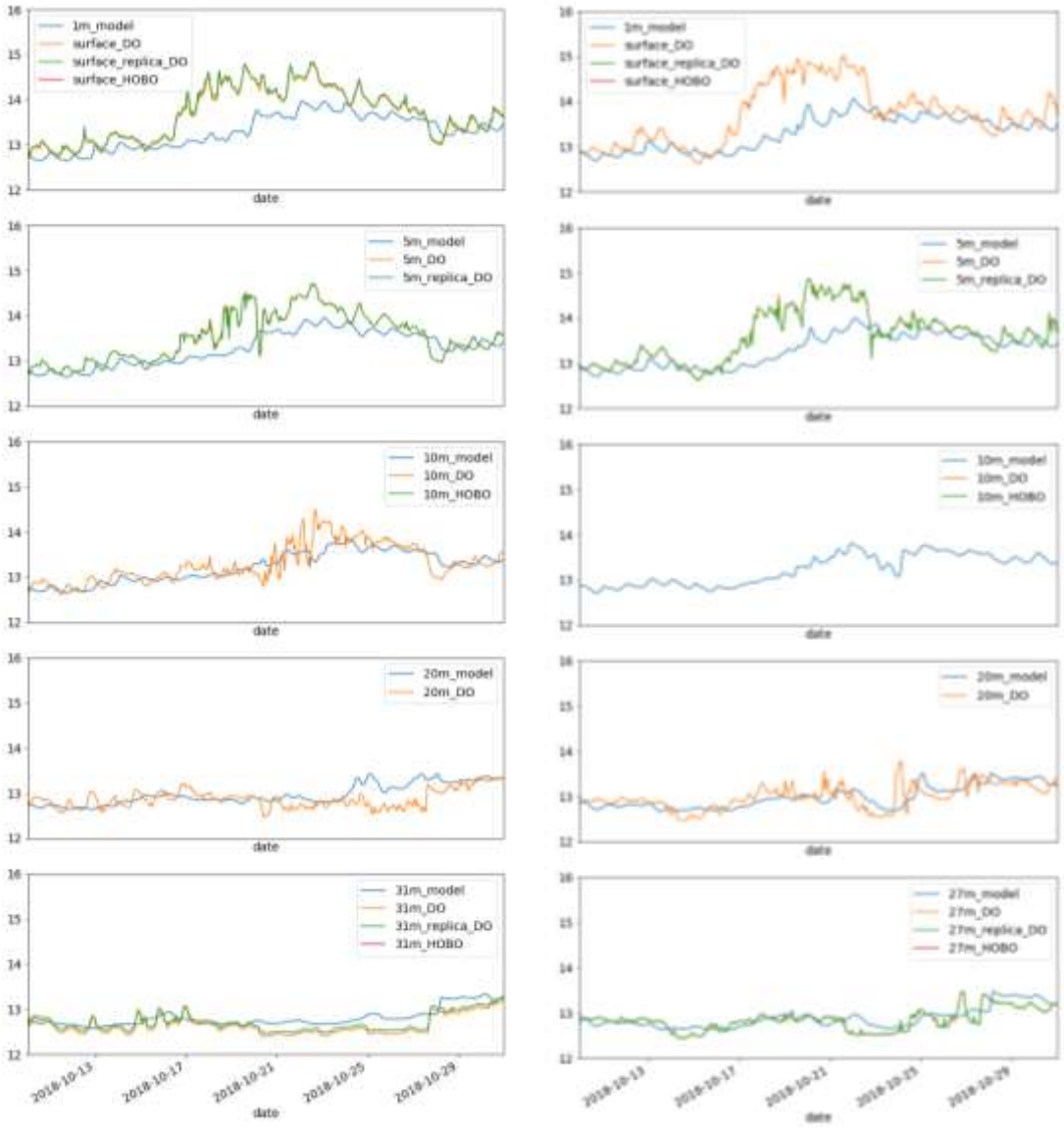

Figure 0.16: Temperature comparison between the observations and the calibrated model at the Site 1 (left) and site 2 (right), during the warming event in October 2018.

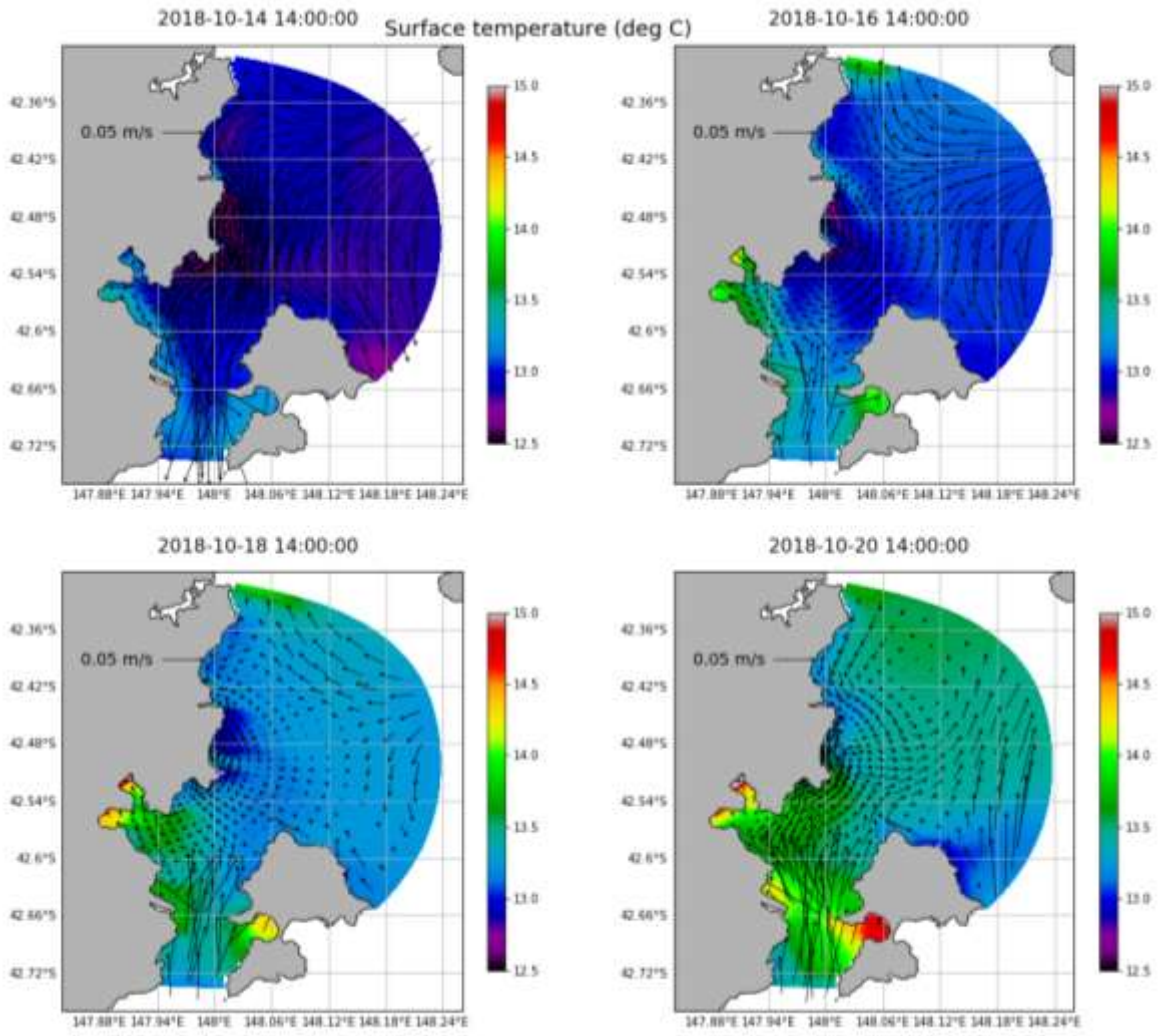

Figure 0.17: Warming event: surface temperature and depth-average currents. The northward flow through Mercury Passage brings relatively warm water to the mooring sites.

Competition between cool and warm water masses

In June and July 2019, the 3 mooring sites show 5-6 oscillations between warmer and colder conditions throughout the water column that are well captured by the OKE model (Figure 4.11). Looking into details into one oscillation between a warm-cold-warm cycle, we can see that there is competition between a warm-water mass originating from Great Oyster Bay and a cold-water mass trapped in the shallow areas along the coast (Figures 4.12 and 4.13).

The warm water mass intrudes the domain through the western (offshore) ocean boundary. When a cyclonic circulation is in place offshore of Okehampton Bay, it pushes warm water in Mercury Passage (top panels Figure 4.12, 17th and 18th of June; bottom panels Figure 4.13, 24th of June). In June, the air-sea fluxes cool down the ocean and the shallow coastal areas are dominated by relatively colder water masses. Depending on the circulation patterns, the cold-water mass either can stay closely trapped along the coast (top panels Figure 4.12, 17th and 18th of June) or can intrude further offshore. On the 19th of June (Figure 4.12), cold water from Chainman's Bay along Maria Island west coast and the opposite bay on the mainland (Carrick-Fergus Bay) are entrained in Mercury passage and move northward. On the 21st (Figure 4.13), the cold tongue reaches Lords Bluff, then the whole northern part of Mercury Passage (Triabunna, Orford,

Spring Bay, Okehampton Bay, northern Maria Island) cools down 1°C on the 22nd of June, until warm water from Great Oyster Bay starts to intrude the area again on the 23rd and 24th of June.

The good representation of the synoptic variations of temperature at the mooring sites via correct transport of water masses during the June/July 2019 period gives us very good confidence in the performance of the model. The competing influence of the Great Oyster Bay circulation and the Mercury Passage circulation on Okehampton Bay water masses is well represented by the OKE model.

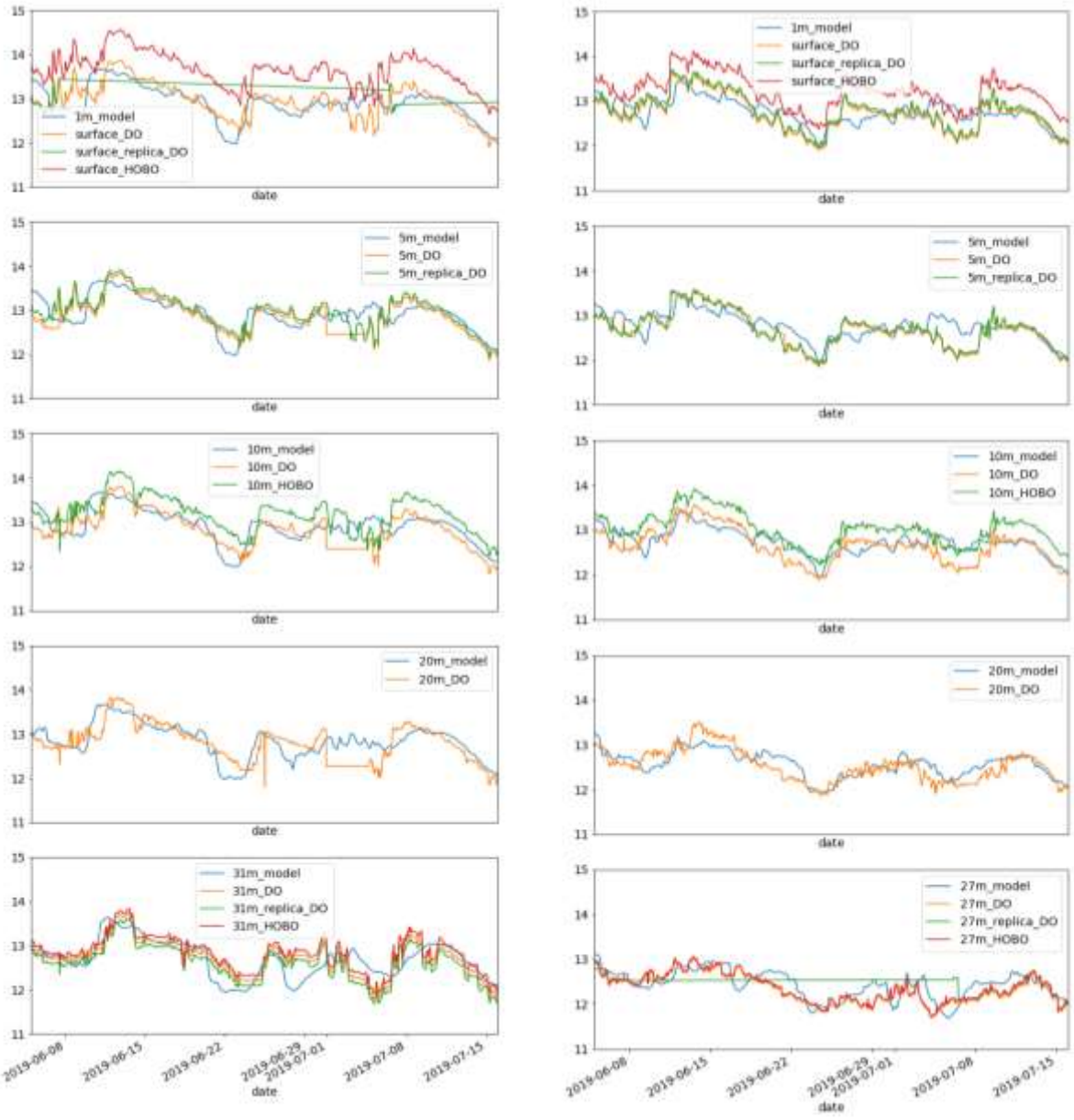

Figure 0.18: Temperature comparison between the observations and the calibrated model at the Site 1 (left) and site 2 (right), during the successive cooling/warming events in June and July 2019.

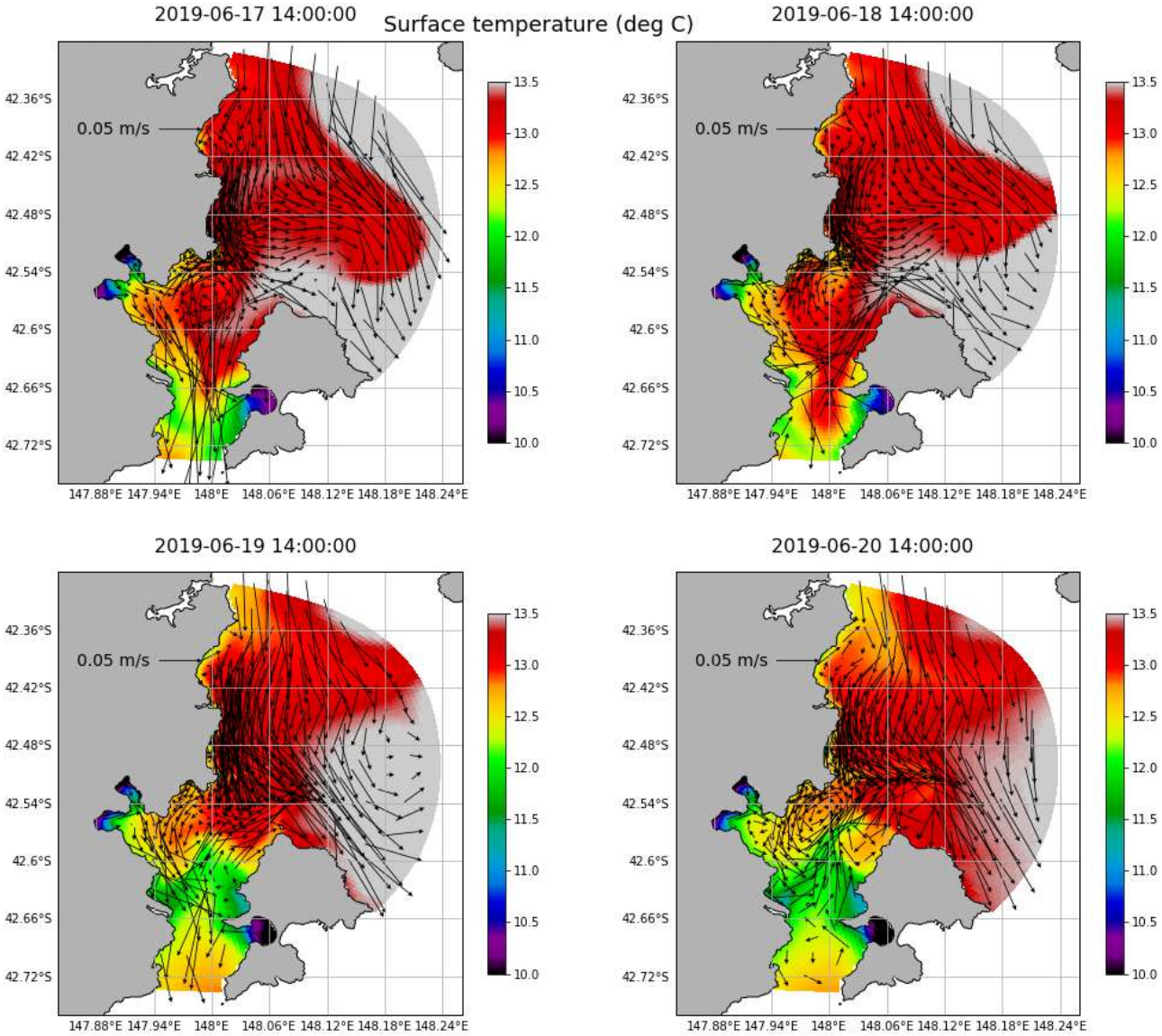

Figure 0.19: Competing circulation patterns affecting temperature in Okehampton Bay: surface temperature and depth-average currents. The northward flow through Mercury Passage brings relatively cold water to the mooring sites, while circulation patterns in Great Oyster Bay bring warm water.

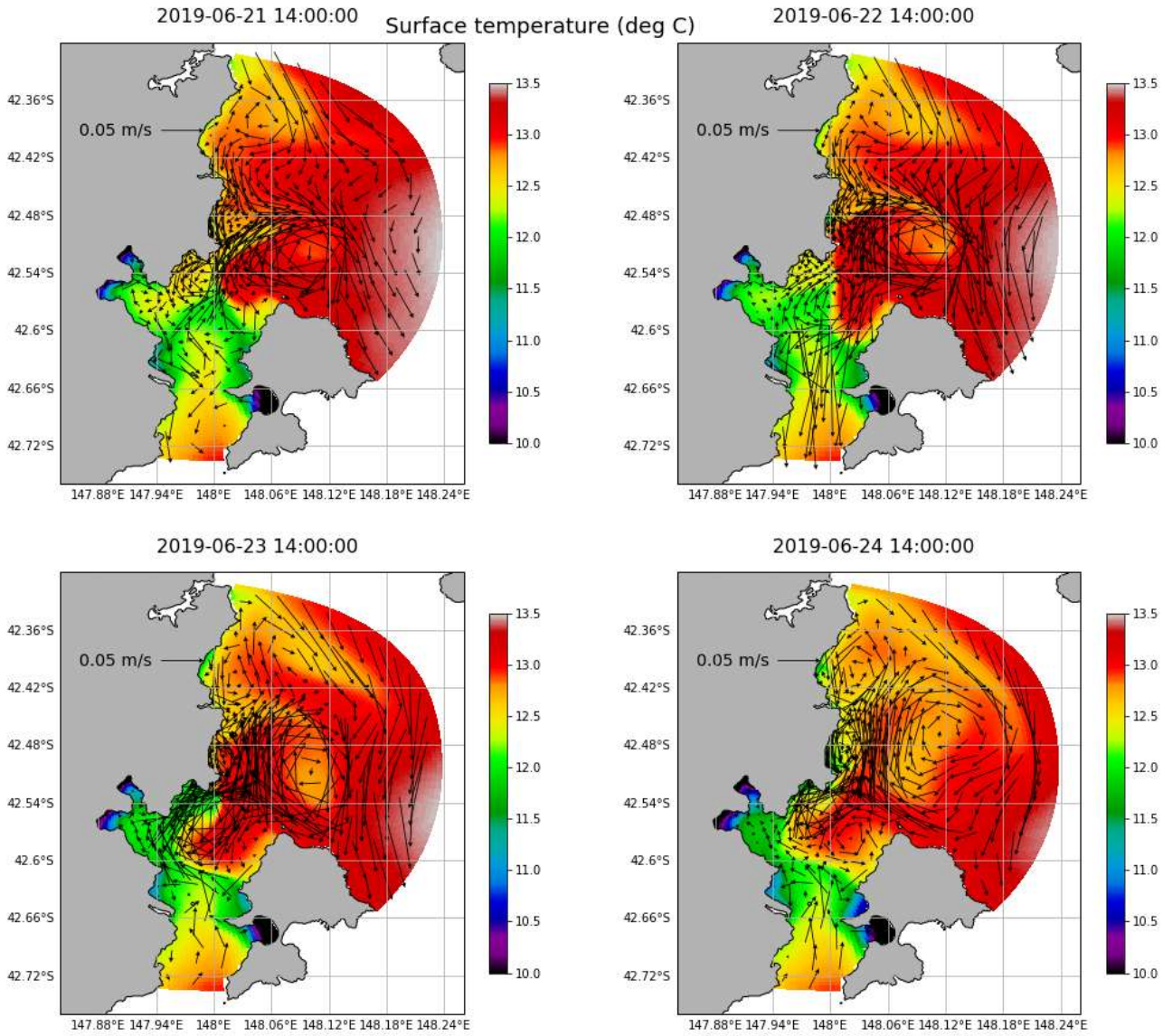

Figure 0.20: same as Figure 4-12 for later dates.

5. Connectivity Analyses

5.1 Methodology - Connectivity Metrics

The model produces predictions of sea level, water properties (temperature and salinity) and currents within the domain of interest. This can be used to produce connectivity analyses. There are different ways to provide insight into how long a dissolved substance is available within a regional water body i.e. maps of residual flow, passive tracer distributions, age tracers and flushing times. The different techniques, their advantages and limitations are described in this section.

Residual flow

The seasonal mean of 3D and 2D currents provides an indication of the long-term fate of tracers within the domain. Since the forcing in Okehampton Bay varies on a seasonal basis, it is instructive to provide residual flow maps capturing this variation.

Sources points - passive tracer at a designated location

The most informative method to diagnose the fate of a pollution source is to supply order statistics of spatial distributions of passive tracer concentration as a result of input at designated locations.

The passive tracer is continuously injected with a unit flux (e.g. 1 kg/s) of material into a layer of the model at a designated grid point. The resulting material is advected and diffused by ambient conditions to provide a spatially and temporally varying distribution of passive tracer (with concentration units kg/m^3). For Okehampton Bay, the passive tracer was injected into a 2m layer near the seabed at a grid point inside the lease area.

The resultant distributions of the passive tracer concentration provide information on where, and in what concentrations water is transported. By providing order statistics (5^{th}, 50^{th} (median) and 95^{th} percentile distributions) based on multi-year runs (2018-2019 for now), we integrate over most forcing conditions the region is subject to, and provide a measure of variability that is experienced. These order statistics are computed from hourly snapshots of surface and bottom layer tracer distributions

The conservation equations describing tracer movement are linear with respect to tracer concentration, so if the actual flux is known the corresponding distributions can be scaled accordingly. For example, it the actual flux was 100 kg/s then all the concentrations in the presented plots would need to be multiplied by a factor of 100.

Note that, the tracer is passive in the sense that it only undergoes advection and mixing as a result of the ambient flow. There are no decay or growth processes included, and to comprehensively understand the impact of marine farming in Okehampton Bay on receiving water quality and sediment dynamics, a calibrated BGC model would be required.

Regions analysis

Flushing times (the non-stationary method, Tartinville et al., 1997), residence times (batch reactor approach, Bailey and Ollis, 1986) and age tracers (Baird et al., 2006) metrics rely on the definition of sub-regions in the domain. We decompose the study area into five regions for this purpose (Figure 5.1) and for which these metrics may be computed.

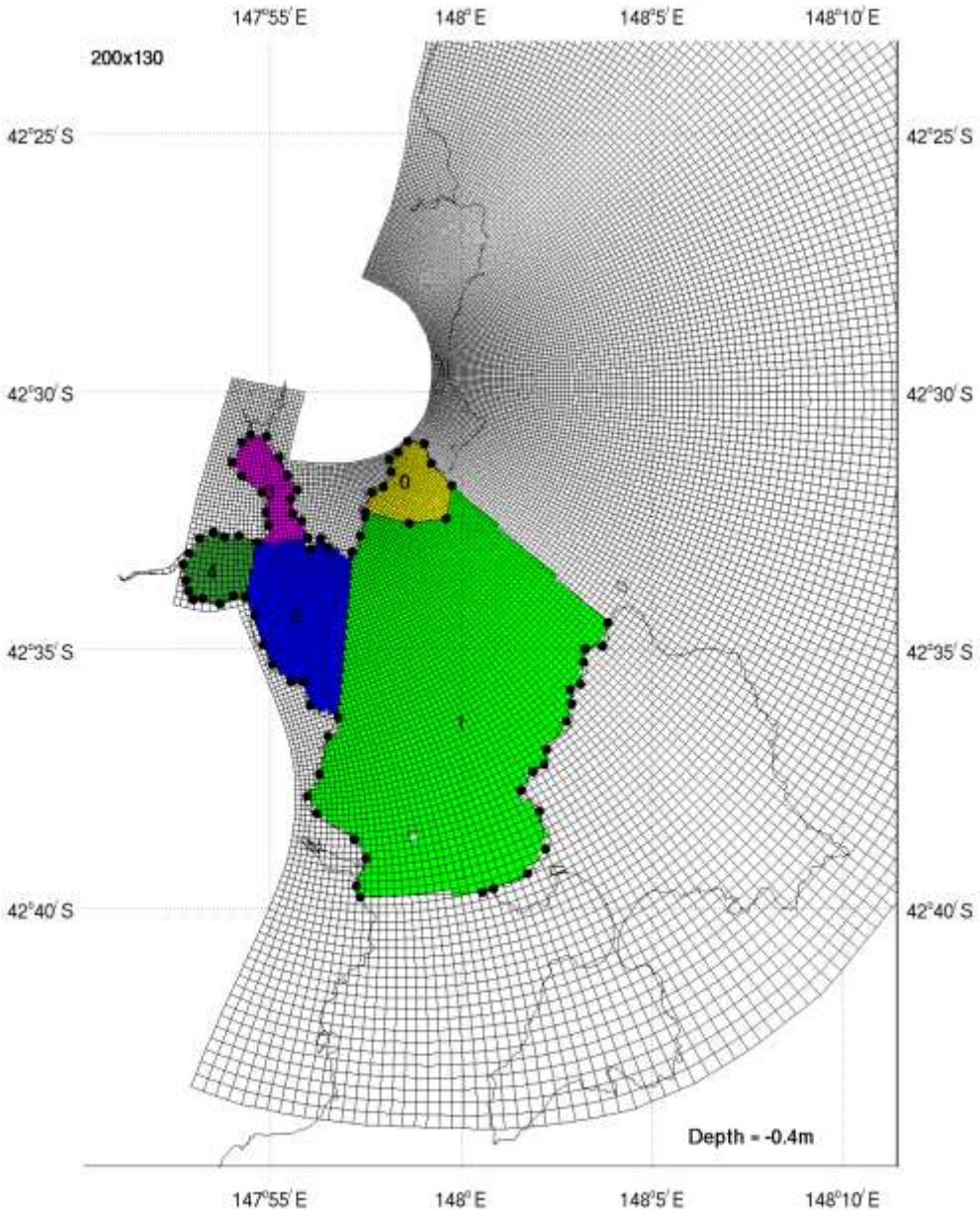

Figure 0.21: Sub-regions used in the connectivity analyses.

Flushing and residence metrics may not always produce reliable results, often providing a large range of values, sometimes with ranges spanning an order of magnitude. These metrics are influenced by the forcing conditions in effect at the time of computation and the size of the region chosen to compute the metric.

Moreover, the assumptions upon which the method is based are often violated, and the presence of tides can unduly bias results.

Caution must be taken when quoting flushing / residence times for a region as they are not always reliable indicators of the absolute time it takes a substance to remain within or exit a region. For example, a strong ebb tide may effectively flush a small region on a semi-diurnal timescale, however, on the flood tide the material is returned to its original position at approximately the same concentration. Also, material may be removed from a designated flushing region to be deposited in a neighbouring region - material remains in the system but this cannot be revealed by a flushing time alone.

Flushing times - non-stationary method (Tartinville et al. 1997)

Sub-region 0 (Okehampton Bay) is initialized with a given concentration and the concentration is set to zero outside of the sub-region. The flushing time is defined as the time for the total mass in the sub-region to decrease by a factor of 1/e (~38%, i.e. the e-folding time).
This representation of the flushing time assumes that tracer is well mixed in the sub-region and the total mass is assumed to decrease exponentially according to:

$$M(t) = M_0 e^{-t/\tau}$$

where M_0 is the initial mass and τ is the flushing time scale. When $M = M_0/e$ then $t = \tau$, hence the flushing time can be recovered.
This diagnostic is highly sensitive to the size of the region chosen and forcing in effect at the time.

Residence time

The residence time may also be computed using the well-mixed batch reactor approach (Bailey and Ollis, 1986), where the residence time is the time it takes a given flux of water to replace a given volume. There exist two possibilities when computing total fluxes between a given region and its neighbours: 1. the instantaneous (one-way) flux may be used; the presence of large tides can create very large oscillating fluxes that turn the region volume over quickly, or 2. the net (incoming plus outgoing) flux. It is possible that simultaneous inflow and outflow through some region boundaries exist, so that even though large volumes of new water are entering the region, the net exchange is small and consequently computed residence times may be very long.

The two approaches to residence time are computed for each day, i.e. it is an average over a day of simulation. These can provide vastly different responses.
The residence time in this context is dependent on the size of the region, and location of adjoining boundaries between regions relative to the circulation. This method does not deliver a robust indication of system connectivity.

Age tracer

Residence time may also be evaluated by considering an ‘age tracer’. The ‘age tracer’ is incremented at a rate of 1 day^{-1} within the sub-region 0 and the rate is set to zero elsewhere.
Tracer within the region is transported out of the region until quasi-steady state is achieved. The value of the age tracer within the region provides an indication of how long it has remained within the region.

Order statistics of the age tracer can provide an indication of the variability of the age of tracer within the region. Again, the age is dependent on the forcing in effect at the time and the location and size of the region boundaries but is considered a better measure of connectivity than the flushing metrics. The 5th percentile age reflects tidal exchanges and the 95th percentile reflects the age resulting from residual circulation.

5.2 Residual flow

The seasonal mean currents, temperature and salinity were all calculated for the calibrated model over the August 2018 to July 2019 period, with December-January-February being the summer season. The depth-averaged currents (Figure 5.2) and surface currents (Figure 5.3) provide an indication of the long-term fate of tracers within the domain. Overall, the results from the calibrated model confirm the findings obtained with the pilot model. However, there is clearly some interannual variation in the predominance of the main circulation patterns and also some variations in seasonal temperature from one year to another. Southward flows are more dominant during the August 2018-July 2019 period compared to the 2016-2017 period.

Near the lease the current is mainly flowing eastward towards Lords Bluff (Figure 5.4). The currents then turn around the bluff toward the north-east. When reaching Plain Place Beach (just north of Lords Bluff), the north-eastward current either keeps flowing northward or meets with a southward flow. In Autumn 2019, this southward flow is stronger than in previous years and meanders closer to the coast, creating a strong south-westward current at the lease site.

In the Great Oyster Bay, the depth-averaged currents show 2 main circulation patterns, already present in the pilot model. The first one is a large cyclonic circulation or northward flow, associated with a northward along shore current and a small anticyclonic re-circulation along Plain Place Beach (Figure 5.2, summer). The second circulation pattern is a strong southward along-shore current that meanders along the coast all the way to Mercury Passage, associated with a large anticyclonic circulation or southward flow in Great Oyster Bay (Figure 5.2) - with a strong southward flow in spring 2018 and autumn 2019, and weaker one in winter with a small anticyclonic re-circulation developing along Plain Place Beach. On average, the current is flowing southward all year round in the southern part of Mercury Passage.

The surface currents (Figure 5.3) show a slightly different picture with strong southward flow in autumn in Great Oyster Bay and Mercury Passage, and strong south-eastward flow in the northern part of Mercury Passage in winter and spring. These depth-average and surface currents mean that there is strong north-westward currents near the bottom in Mercury Passage, with upwelling at the coast and downwelling along Maria Island.

These results from the calibrated model confirm the findings obtained with the pilot model. They indicate that any passive tracer released near the lease is more likely to be first transported towards Lords Bluff. Once at the Bluff, the tracer can either recirculate off Plain Place Beach, or deviate to the south, with stronger southward deviation in 2018-2019 in comparison to 2016-2017. There is likely to be important re-suspension where upwelling occurs along the coast.

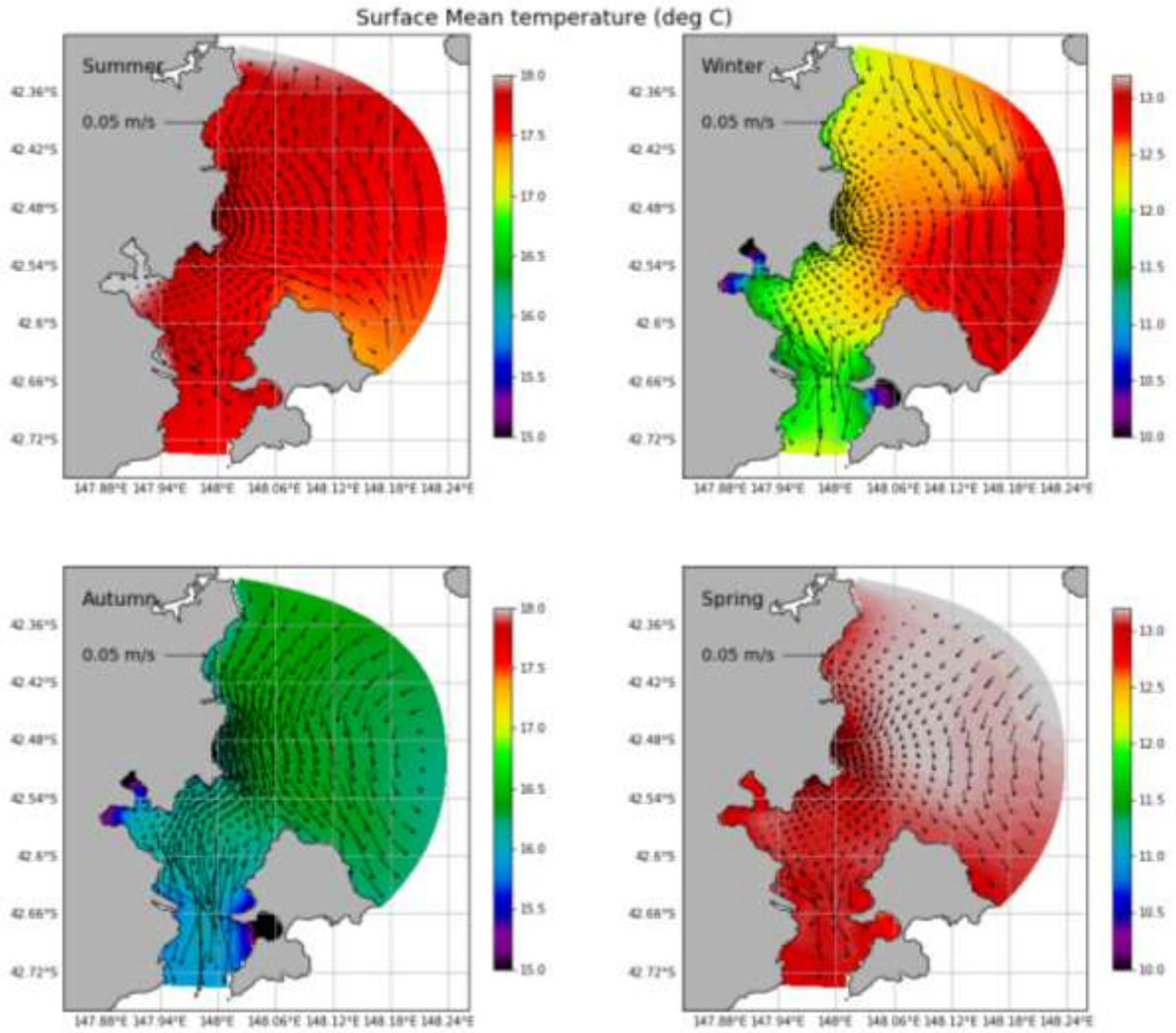

Figure 0.22: Aug 2018- July 2019 seasonal conditions of the OKE model: seasonally-average and depth-averaged circulation and surface temperature.

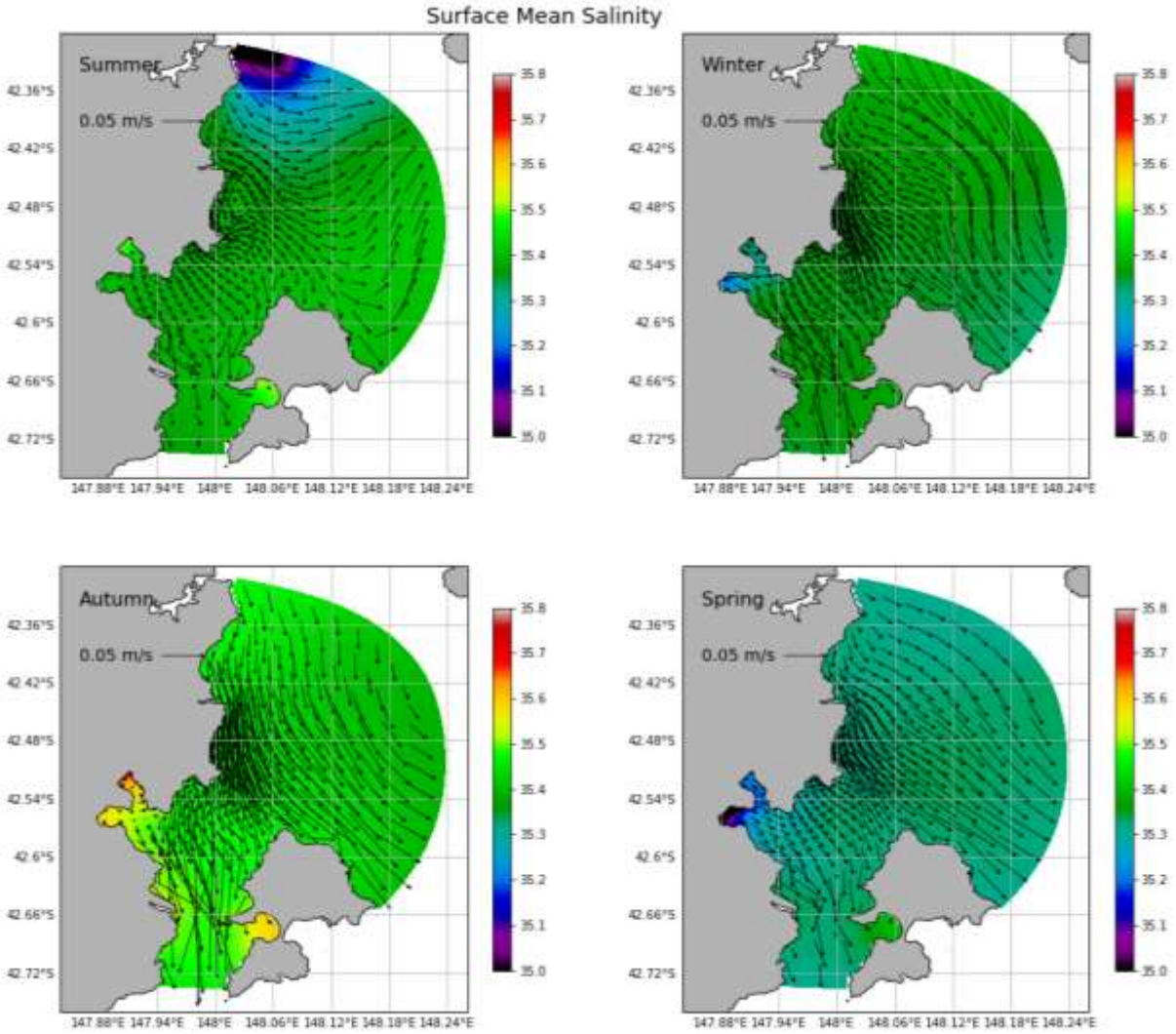

Figure 0.23: Aug 2018- July 2019 seasonal conditions of the OKE model: seasonally-average surface circulation and surface salinity.

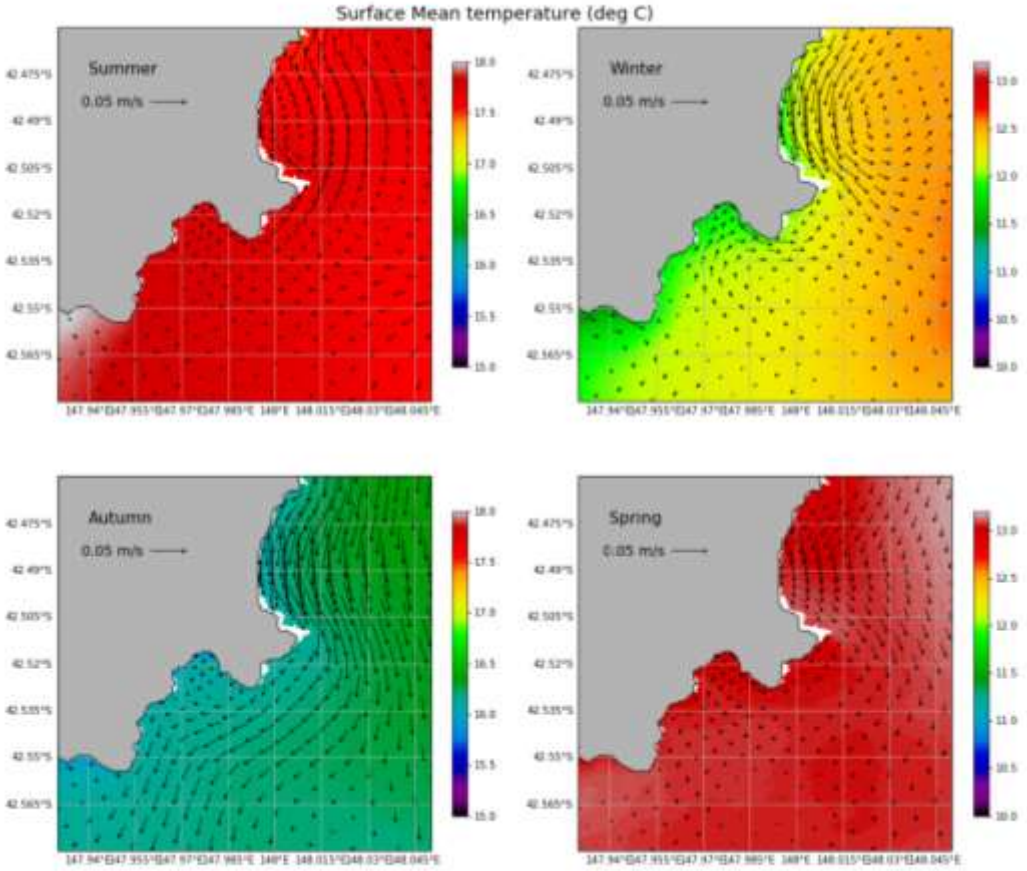

Figure 0.24: Aug 2018- July 2019 seasonal conditions: same as Figure 5.2 but with a zoom around Okehampton Bay.

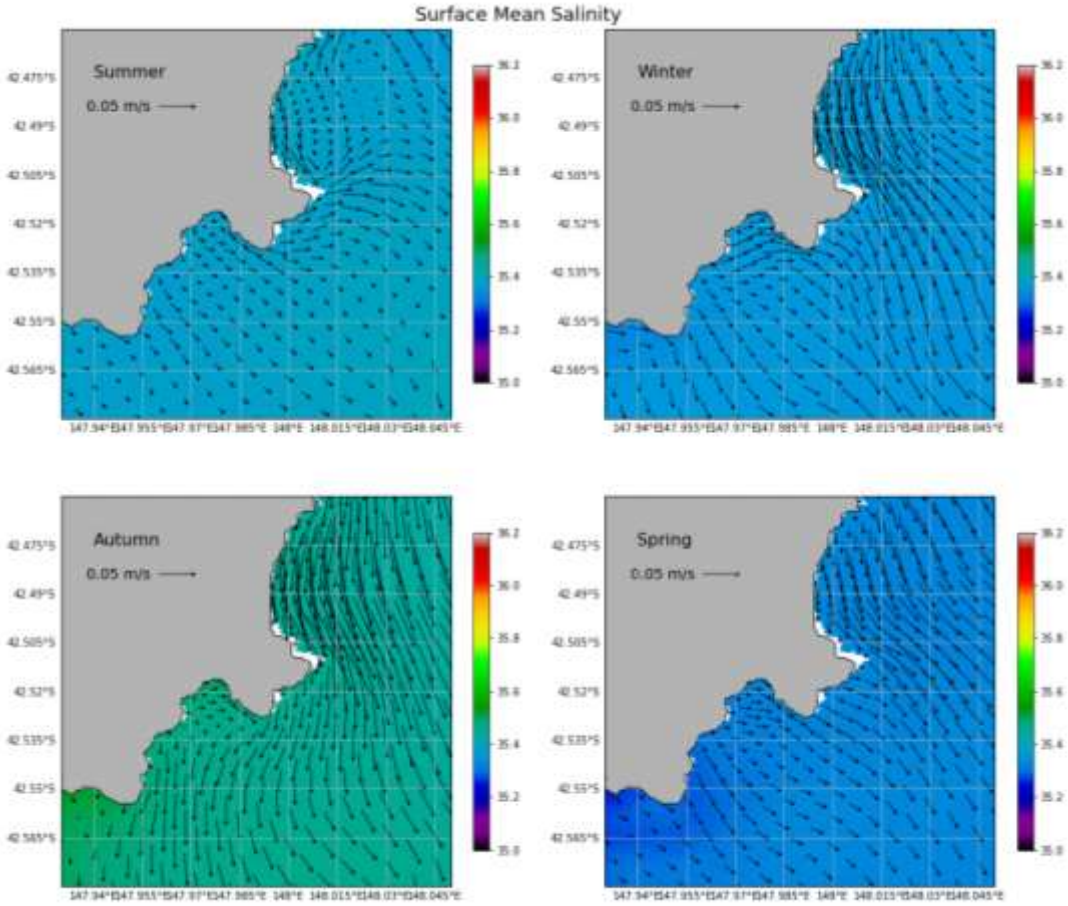

Figure 0.25: Aug 2018- July 2019 seasonal conditions: same as Figure 5.3 but with a zoom around Okehampton Bay.

5.3 Source point inside the Okehampton Bay lease

Passive tracer was injected at a rate of 1 kg/s in a 2m layer near the seabed at (147.98°E, -42.53°S) (black dot on Figure 5.8). This point source is located inside the lease where the water depth is approximately 25m. The passive tracer was advected by the 3D currents provided by the calibrated model over the August 2018 to July 2019 period. To summarize the behaviour of this bottom release, order statistics were computed from hourly snapshots of surface and bottom layer tracer distributions. The 5th, 50th and 95th percentile distributions provide information on where, and in what concentrations the passive tracer was transported over this 1-year period.

Far field

The bottom release of passive tracer resulted in spatial distributions of the bottom and surface concentrations that look quite similar in Mercury Passage and Great Oyster Bay, with high concentration in shallow areas and well mixed tracer offshore (Figures 5.6 and 5.7; note that the colour-bars are identical between figures but differ for each of the order statistics). In the bottom layer, the plume of high concentration is more trapped along the 35 to 40m isobaths.

The bottom and surface median distributions are displayed in Figures 5.6 and 5.7 middle panel (50th percentile). Unsurprisingly, the highest concentration of tracer is found in Okehampton Bay in the immediate vicinity of the release site. On average, the plume of high tracer concentration is transported

more southward than northward along the coast over the August 2018 - July 2019 period. To the north, the plume reaches Plain Place Beach but does not reach the area north of Little Swanport. To the south it reaches Triabunna, Orford and Spring Beach as well as Mercury Passage. The propagation is consistent with the residual flow analysis above, with mean northward flow in summer, winter and spring near the lease and southward flow in autumn. Despite the fact that the southward flow is not the predominant flow at the lease, the southward plume of passive tracer is the dominant pattern. There are two reasons for this; first, the circulation offshore of the lease is predominantly southward, and secondly, the residence time near Triabunna, Orford and Mercury Passage is higher than in Great Oyster Bay. In other words, while the currents push the passive tracer less often to the south, once the tracer reaches the southern areas, it gets trapped and stays for a longer period.

In comparison with the 2016-2017 pilot model analysis, the southward flow occurs more often during the August 2018- July 2019 period, demonstrating the interannual variability of the occurrences of the main large circulation patterns in the area and their impact on the tracer distribution.

Near Triabunna, Orford and Spring Beach, the bottom and surface concentration are similar, with median concentrations of 0.6-0.7x10^{-3} kg/m^3, which varies from 0.02-0.1x10^{-3} kg/m^3 (5^{th} percentile) to 1.3-1.5x10^{-3} kg/m^3 (95^{th} percentile). The conservation equations describing tracer movement are linear with respect to tracer concentration, so if the actual flux is known the corresponding concentrations can be scaled accordingly.

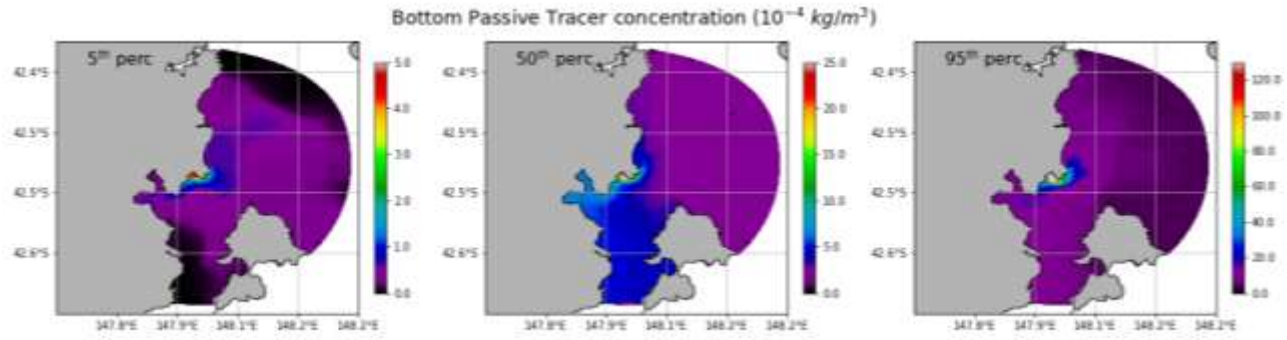

Figure 0.26: Bottom distributions of tracer concentration (in kg/m3) due to 1kg/s flux into a 2m layer near the bottom of the lease (black dot in Figure 3.7): 5th (left), 50th (middle) and 95th (right) percentile distributions. Note that the colour bar is the same as in Figure 5.7.

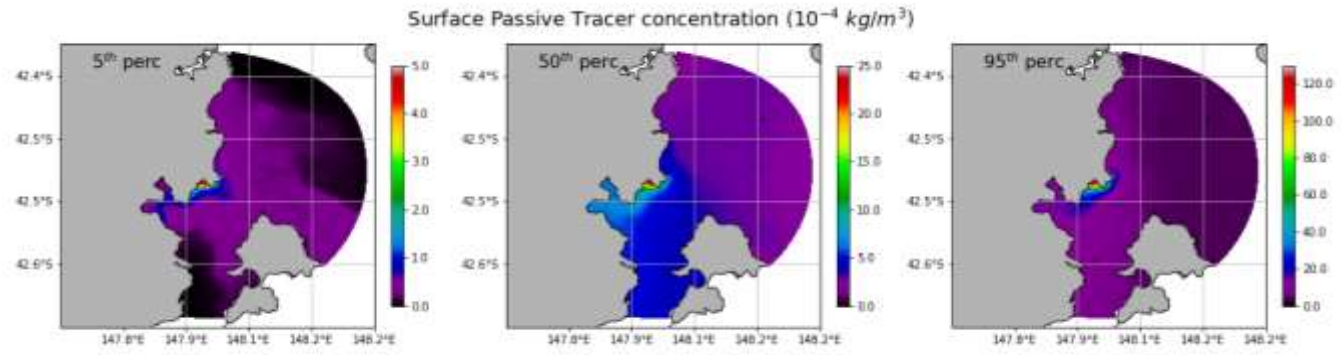

Figure 0.27: Surface distributions of tracer concentration (in kg/m3) due to 1kg/s flux into a 2m layer near the bottom of the lease (black dot in Figure 3.7): 5th (left), 50th (middle) and 95th (right) percentile distributions. Note that the colour bar is the same as in Figure 5.6.

Okehampton Bay

In Okehampton Bay and near the lease area, the spatial distributions of the bottom and surface concentrations, resulting from the bottom release, show more differences (Figures 5.8 and 5.9) (note that the colour-bars are different). As the release of the tracer occurs at the bottom, highest concentrations are found in the vicinity of the point source at the bottom with a median concentration of 0.12 kg/m^3 which varies from 0.04 to up to 0.38 kg/m^3 (5th and 95th percentile at the point source). At the surface, the highest concentrations are found along Okehampton Beach and are two orders of magnitude smaller than the highest concentrations of the bottom field, with a median concentration of 0.3x10^{-2} kg/m^3, which varies from 0.05x10^{-2} to up to 1.9x10^{-2} kg/m^3 (maximum value of the 5th and 95th percentile along Okehampton Beach). This is indicative of a 2-layer type flow that is not dominated by vertical mixing. Tracer is advected a few hundred of meters from the source point before it hits the surface.

Along Okehampton Beach and Reids Beach, the bottom and surface concentrations are similar, highlighting that the tracer is rapidly mixed over the entire water column once transported away from the source point. The tracer distribution in Okehampton Bay is similar to the 2016-2017 pilot model analysis, giving high confidence in this analysis. Again, if the actual flux is known, the corresponding concentrations can be scaled accordingly.

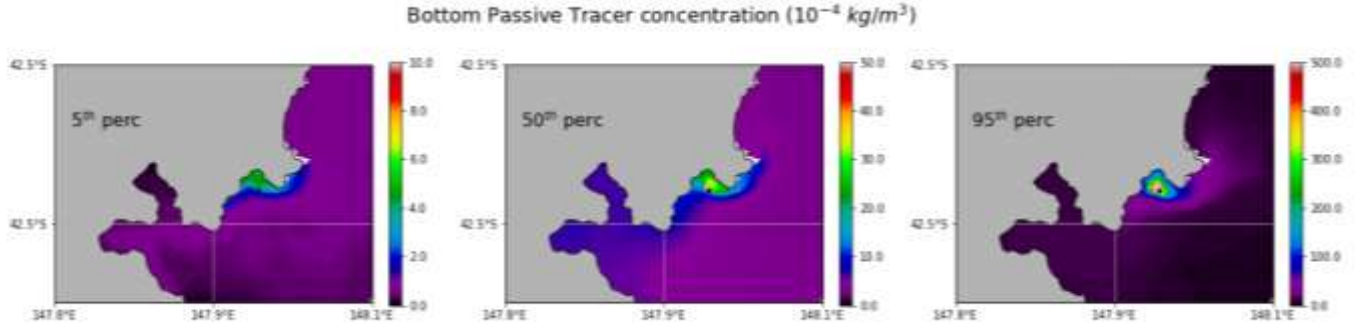

Figure 0.28: Bottom distributions of tracer concentration (in kg/m3) due to 1kg/s flux into a 2m layer near the bottom of the lease (black dot): 5th (left) , 50th (middle) and 95th (right) percentile distributions. Note that the colour bar is different than that in Figures 5-6, 5-7, 5-9.

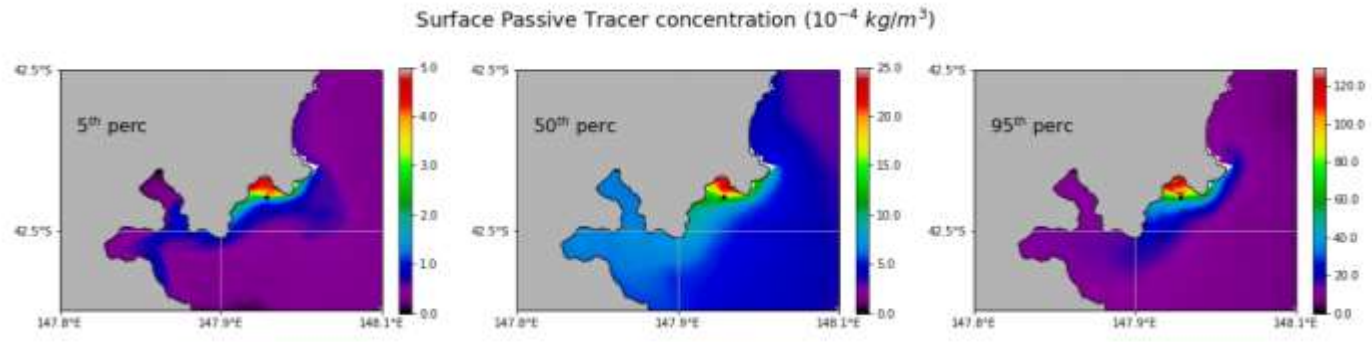

Figure 0.29: Surface distributions of tracer concentration (in kg/m3) due to 1kg/s flux into a 2m layer near the bottom of the lease (black dot): 5th (left) , 50th (middle) and 95th (right) percentile distributions. Note that the colour bar is the same as that in Figure 5.6, but different than Figure 5.8.

5.4 Region analysis

Flushing and residence times in Okehampton Bay

The various metrics described in Section 5.1.3 are often used as an indicator of how long material is retained in a system. These metrics are, however, dependent of the size of the region being considered as well as the forcing in effect at the time. Also, assumptions on which some of the metrics are founded are often violated in reality (e.g. uniform distribution of material within the region). Due to these reasons these metrics should be used with caution. Residence times attempt to provide insight into how long a dissolved substance is available within a regional water body; more and better information can be provided by supplying order statistics of spatial distributions of passive tracer concentration due to input at designated locations, hence the analysis of Section 5.3. is considered a more definitive diagnosis of where material goes, in what quantities it goes there and what the variability of those quantities are. We do, however, include values of flushing for completeness below.

The flushing and residence times were computed using Okehampton Bay and the lease as a single region (Region 0, Figure 5.1).

The flushing and residence times are dependent on the size of the region. Region 0 being a relatively small region, the flushing times are short and vary from 0.2 to 3.9 days (Table 5.1). The residence times using the instantaneous flux are similar and vary from 0.2 to 1.8 days. As predicted, the instantaneous flux residence time is very small in comparison to the residence using net fluxes, with the maximum value looking unreasonably large. Again, these methods do not always deliver a robust indication of system connectivity.

Table 0.4: Connectivity metrics (days) in Okehampton Bay region 0 for various methodologies.

Metrics (days)	**Median Value (min - max)**
Flushing time	1.3 (0.2 - 3.9)
Residence time – instantaneous flux	0.7 (0.2 – 1.8)
Residence time – net flux	87 (2 – 6,527)
Particles residence time	*

*particles tracking was not performed for this report.

Age tracer

Residence time in Okehampton Bay was also evaluated by considering an 'age tracer' inside Region 0 (Figure 5.1 and Figure 5.10).

We computed order statistics from hourly snapshots of surface distribution of the age tracer. The 5th, 50th and 95th percentile distributions provide an indication of the variability of the residence within Okehampton Bay (Figure 5.10). The age is not uniform in Region 0, with higher residence time near Okehampton Beach. The median age in Okehampton Bay is around 1 to 2 days, which is in line with the computed flushing times.

Again, the age is dependent on the forcing in effect at the time and the location and size of the region boundaries. Region 0 being a relatively small region, the age is small, with the longest tracer age not exceeding 4 days.

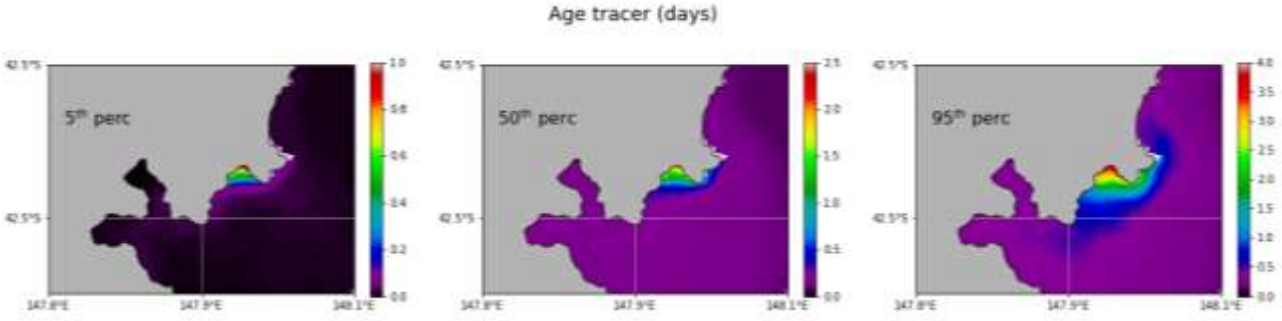

Figure 0.30: Surface distributions of the age (in days) of a tracer incremented at a rate of 1 day^{-1} within Okehampton Bay region: 5th (left), 50th (middle) and 95th (right) percentile distributions. Region 0 is delimited by the black line and black points.

6.Summary

The CSIRO Costal Environment Modelling team (CEM team) developed a hydrodynamic model to investigate the far-field and regional hydrodynamic connectivity around Okehampton Bay and the Mercury Passage surrounds: the OKE model. This report describes the development of the OKE calibrated model, its application over the August 2018 - July 2019 period, plus background knowledge of the area, description of the model and observations, calibration and assessment of the model, and information of the connectivity characteristics within the near and far-field of Okehampton Bay.

OKE model calibration

The high-temporal and spatial temperature observations allowed us to calibrate the model to satisfactory standard. The resulting calibrated model shows very good statistical skill in temperature and sea-level. Despite the absence of salinity observations, we think that the Prosser River discharge plays an insignificant role in the circulation in Okehampton Bay and Mercury Passage during the calibration period. Additionally, we were able to correlate some synoptic variability of temperature at the mooring sites with dynamical processes (intrusions of offshore water and influence of shallow areas), which gives us good confidence in the performance of the model in representing the complex circulation in Mercury Passage.

Connectivity analysis

While the flushing and residence metrics show a quick turn-over in Okehampton Bay, these are not the best metrics to understand where and in what quantities tracers are transported by the currents around the lease. The distributions of passive tracer, along with the seasonal residual flow analysis, provide the best picture to understand connectivity near Okehampton Bay and the Mercury Passage surrounds.

From a circulation point of view, there are two main circulation patterns near Okehampton Bay:

- a northward along shore current associated with a small anticyclonic re-circulation along Plain Place Beach ; this circulation pattern is sometimes associated with a large cyclonic circulation in Great Oyster Bay ; near the lease, the current is then flowing eastward towards Lords Bluff

- a strong southward along-shore current that meanders along the coast all the way to Spring Bay and Mercury Passage, associated with a large anticyclonic circulation in Great Oyster Bay; depending on the position of the meander, the current near the lease flows either south-westward toward Orford as part of the meander flow, or eastward towards Lords Bluff before merging with the southward meandering flow.

There is some interannual variability in the predominance of one pattern or another.

The passive tracer analysis shows that the plume of high tracer concentration is trapped along the coast in shallow areas. At the lease, the currents push tracers less often to the south and into Triabunna and Orford, and more often to the north. However, the southward meandering circulation can deflect the tracer towards the south offshore of the lease. Moreover, as the tracer stays trapped near Triabunna, Orford and Spring Beach for longer periods than in Plain Place Bay, the median concentration south of the lease is higher than north of the lease in 2018-2019.

In Okehampton Bay, the highest concentrations are found near the source point at the bottom of the lease. At the surface, the tracer tends to get trapped along Okehampton Beach (north-east part of Okehampton Bay) with a median tracer concentration of 0.3×10^{-2} kg/m^3 which is ~2.5% of the median concentration found at the source point. The high concentration plume is transported almost equally northward and

southward of the lease along the coast, with a median tracer concentration of $0.08x10^{-2}$ kg/m^3 at 5 km distance from the 1 kg/s source point.

7. Extension and Adoption

The outcomes of this project have been incorporated into the management decisions of the EPA to inform regulation of the salmon farming lease within Okehampton Bay.

8. Project materials developed

The profiler buoy obtained through this program has been redeployed to support ongoing work in South East Tasmania and will be a valuable addition to monitoring in Storm Bay and any future FRDC supported modelling programs.

9. References

Bailey, J.E., Ollis, D.F., (1986) Biochemical engineering fundamentals. McGraw-Hill Book Company, New York, 984pp.

Baird, M., Timko,P., Suthers,I., Middleton,J.H., (2006) Coupled physical–biological modelling study of the East Australian Current with idealized wind forcing. Part I. Biological model inter-comparison. J. Mar. Syst. 59, 249–270.

Blumberg, A.F. , Herring, J. (1987) Circulation modelling using orthogonal curvilinear coordinates

Nihoul, J.C.J. , Jamart , B.M. (Eds.), Three-Dimensional Models of Marine and Estuarine Dynamics, Elsevier

Herzfeld, M. (2006). An alternative coordinate system for solving finite difference ocean models. Ocean Modelling, 14(3), 174– 196.

Langlais, C., Andrewartha, J., Herzfeld M. (2019). Okehampton Bay modelling: hydrodynamics and connectivity . Progress Report April 2019.

Oliver, E.C.J., Holbrook, N.J. (2018), Variability and Long-Term Trends in the Shelf Circulation Off Eastern Tasmania, Journal of Geophysical Research. Oceans 123 (10), 7366-7381

Oliver, E.C.J, Herzfeld, M., Holbrook , N.J., (2016) Modelling the shelf circulation off eastern Tasmania, Continental Shelf Research, 130, 14-33

Pilo, G. S., P. R. Oke, T. Rykova, R. Coleman, and K. Ridgway (2015), Do East Australian Current anticyclonic eddies leave the Tasman Sea, J. Geophys. Res. Oceans, 120, 8099–8114, doi:10.1002/2015JC011026.

Ridgway, K. R. (2007), Seasonal circulation around Tasmania: An interface between eastern and western boundary dynamics, J. Geophys. Res., 112, C10016, doi:10.1029/2006JC003898.

Sloyan, B. M., & O'Kane, T. J. (2015). Drivers of decadal variability in the Tasman Sea. Journal of Geophysical Research: Oceans, 120, 3193– 3210. https://doi.org/10.1002/2014JC010550

Tartinville, B., Deleersnijder, E., Rancher, J. (1997) The water residence time in the Mururoa atoll lagoon: sensitivity analysis of a three-dimensional model. Coral Reefs, 16, 193 – 203.